This non-peer reviewed preprint has been submitted for publication in Journal of Geodynamics. Subsequent versions of the manuscript may be somewhat different.

Stress interactions between earthquakes and volcanoes in South Iceland: Application to Eyjafjallajökull and Katla

Trine H. Simmenes[a], Agust Gudmundsson[b*]

[a]Department of Earth Science, University of Bergen, Allegt. 41, NO-5007 Bergen, Norway

[b*]Department of Earth Sciences, Royal Holloway University of London, Egham TW20 0EX, United Kingdom

Abstract

South Iceland contains some of Iceland´s best-known volcanoes (Hekla, Katla, and Eyjafjallajökull) as well as one of its two main seismic zones, namely the South Iceland Seismic Zone (SISZ). The part of the SISZ that produces continuous microseismicity is a 70-km-long and 10-20-km wide zone, located between the active volcanic zones referred to as the West Volcanic Zone and East Volcanic Zones. The largest earthquakes in the SISZ, however, exceed M7, during which the N-S extension of the SISZ may be as wide as 60 km. The SISZ is partly covered with Holocene lava flows where the seismogenic faults occur as dextral NNE-trending and sinistral ENE-trending conjugate arrays. The same fault-segment trends occur in the Pleistocene rocks north of the Holocene lava flows. There are three main stratovolcanoes/central volcanoes located at lateral ends of the SISZ. These are Hekla, which is located in a quadrant of transtension, and Hengill and Eyjafjallajökull, which are located in quadrants of transpression. In the past decades, all these volcanoes have been subject to unrest and two have erupted, namely Hekla in 2000 and Eyjafjallajökull in 2010. The fourth volcano discussed here, Katla, is located just east of Eyjafjallajökull. Here we analyse the stress interaction between the SISZ and these four volcanoes. We provide new numerical models of the effects of seismogenic faulting in the SISZ on the state of stress in the volcanoes, with a particular focus on Eyjafjallajökull and Katla. The results indicate that the general stress transfer from the SISZ to the volcanoes Hengill, Eyjafjallajökull and Katla was primarily compressive and unfavourable for volcanic eruptions prior to the two June 2000 in the SISZ. Magma intrusions into Eyjafjallajökull in the 1990s thus resulted in sill formation and no eruption. There may also have been magma intrusion into Hengill in the 1990s, but no eruption occurred. Prior to the June 2000 earthquakes Hekla was subject to large tensile stress and had frequent eruptions, but the earthquakes resulted in the stress field becoming less tensile and Heklas has not erupted. By contrast, the stress field in Eyjafjallajökull became more tensile following the June 2000 earthquakes so as to favour dike propagation to the surface. Thus, renewed magma intrusion into the volcano in 2009 and early 2010 resulted in two eruptions in Eyjafjallajökull: an effusive eruption in March, and an explosive eruption in April 2010.

Keywords eruptions and earthquakes, dike injection, sill injection, crustal stress, volcanotectonic modelling, seismotectonic modelling

*Coresponding author (Agust.Gudmundsson@rhul.ac.uk)

1. Introduction

The active volcanic zones of Iceland are connected to two mid-ocean ridges: the Reykjanes Ridge in the south and the Kolbeinsey Ridge in the north (Fig. 1). Each connection or junction occurs along an ocean-ridge discontinuity. In South Iceland, the discontinuity is the South Iceland Seismic Zone (SISZ). In north Iceland, and offshore, the discontinuity is the Tjörnes Fracture Zone (TFZ), primarily its main structure, the Husavik-Flatey Fault (HFF). Both the SISZ and the TFZ are the sites of brittle crustal deformation, including strike-slip faulting, normal faulting, and high seismicity (Gudmundsson, 1995a, 2007; Arnadottir et al., 2008; Einarsson, 2008; Jakobsdottir, 2008; Gudmundsson, 2025a,b). The largest earthquakes in Iceland reach estimated magnitudes of M7.1-7.3; they occur on strike-slip faults in the SISZ and the TFZ.

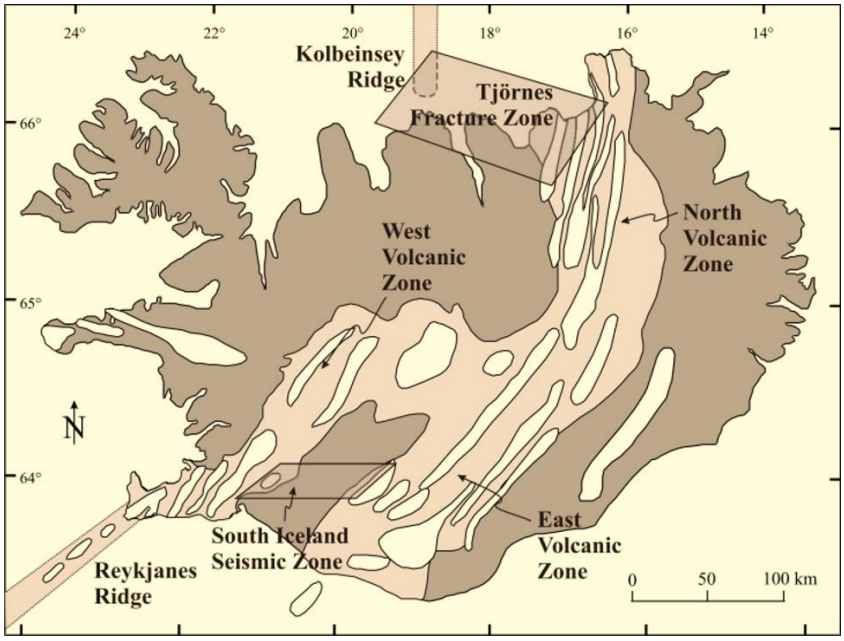

Fig. 1. General geological map of Iceland, which is located at the junction between two ocean ridges: the Kolbeinsey Ridge in the north and the Reykjanes Ridge in the southwest. The connections between the ridges and the volcanic zones of Iceland are through transform zones: the Tjörnes Fracture Zone in the north, whose main transform fault is the Husavik-Flatey Fault (Gudmundsson, 2007), and the South Iceland Seismic Zone (SISZ), in the south.

In this paper the focus is on the SISZ and its interaction with its nearby central volcanoes. The nearby central volcanoes are Hekla, Hengill, and Eyjafjallajökull (Figs. 1, 2). The volcano Katla is to the east of Eyjafjallajökull but may also be affected by stress transfer from the SISZ. The most recent strong earthquakes in the SISZ occurred in the year 2000 when two M6.6 (surface magnitude) earthqukaes occurred on 17 and 21 of June (Jakobsdottir, 2008). A further strong earthquake (M6.3) occurred in the westernmost part of the SISZ in May 2008 (Arnadottir et al., 2008; Sigbjörnsson et al., 2009; Decriem and Arnadottir, 2012). For several years prior to the June 2000 earthquakes, there was large-scale crustal deformation in the two volcanoes located in the quadrants of transpression, namely Hengill and Eyjafjallajökull (Figs. 2, 3). The crustal deformation included compression, uplift and intense earthquake swarms, with some events exceeding M4. Most of this earthquake activity came to an end following the June 2000 earthquakes. An additional indication of crustal deformation related to the ends of the SISZ is that the volcano Hekla, located in one of the quadrants of transtension (Fig. 3), erupted unusually frequently from 1970 and up to 26 February 2000 (Thordarson and Larsen, 2007; Thordarson and Hoskuldsson, 2008) but not at all in the 25 years since the June 2000 earthquakes.

While Hengill and Hekla have been comparatively inactive in the 25 years following the June 2000 earthquakes (apart from the 2008 M6.3 earthquake southeast of Hengill), there were earthquakes and associated deformation in Eyjafjallajökull from time to time between 2005 and 2009 (Sigmundsson et al., 2010; Gudmundsson et al., 2012). These were followed by an intensive earthquake activity and doming in Eyjafjallajökull which began in January 2010 and led up to a small basaltic effusive flank eruption from 20 March to 12 April. After a two-day interval, a new and explosive eruption started on 14 April from the summit of Eyjafjallajökull resulting in a major disruption of air traffic in Europe over many days. Katla has erupted frequently in historical time (the past 1100 years in Iceland) and is expected to erupt again in the coming years. Katla has had much annual seismic activity, which increased somewhat during and following the 2010 Eyjafjallajökull eruptions. However, there has been no major eruption in Katla since 1918.

Here we explore the interaction between stresses and faulting in the SISZ and the nearby volcanoes. We discuss briefly the effects of stress transfer and changes on Hengill and Hekla, but the main focus is on new numerical models showing the stress effects of nearby faulting in the SISZ on Eyjafjallajökull and Katla. In particular, we consider the stress changes generated by the June 2000 earthquakes and how they affected the local stresses in Eyjafjallajökull and Katla. We present numerical models on the stress effects, including also future scenarios where

larger earthquakes than the 2000 earthquakes (e.g., M7-7.1 earthquakes) are likely to occur in the SISZ. Although the focus is here on interaction between seismogenic faulting and magma chambers, the results are perfectly general and apply, with suitable modifications, to interaction between faults and fluid-filled reservoirs of any type.

2. The South Iceland Seismic Zone

Many recent papers and books published in the past decades discuss the structural geology and tectonics of the SISZ (Bergerat et al., 1998; Bergerat, 2001; Bergerat and Angelier, 2001; Bergerat et al., 2003; Gudmundsson and Brenner, 2003; Angelier et al., 2004a,b; Gudmundsson, 2007; Bergerat and Angelier, 2008; Solnes et al., 2013; Gudmundsson, 2017). There have also been many papers on the recent deformation and seismicity of the SISZ (Perlt and Heinert, 2006; Arnadottir et al., 2008; Einarsson, 2008; Jakobsdottir, 2008; Parameswaran et al., 2020, 2023) where more details can be obtained.

In the past 800 years, the SISZ has been subject to destructive earthquakes at least 33 times (Stefansson et al., 1993; Rognvaldsson, 1994; Bergerat, 2001). The data, mainly from the past several centuries, indicate that there are earthquake sequences at intervals of 80-100 years

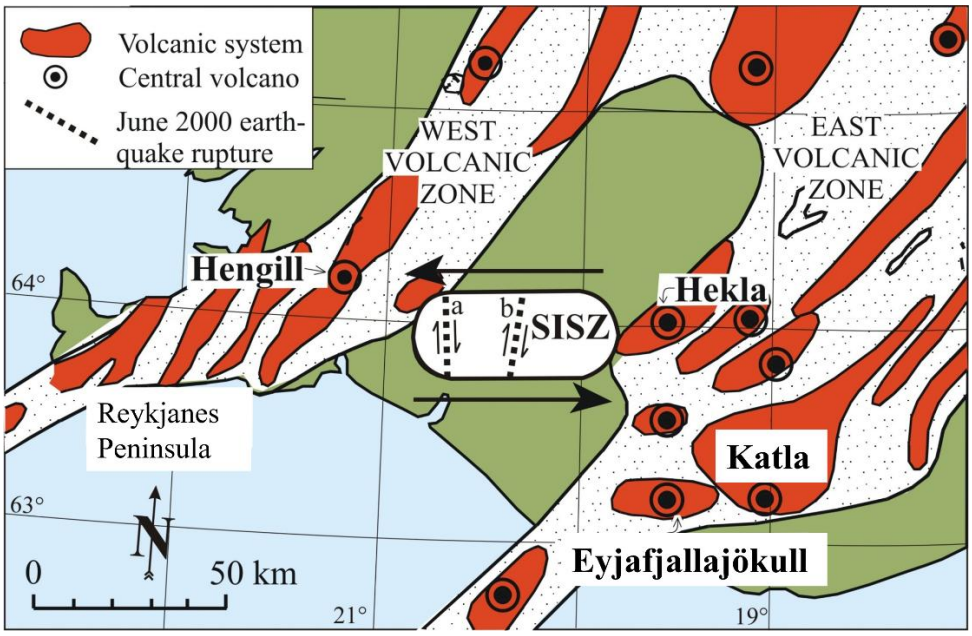

Fig. 2. South Iceland Seismic Zone (SISZ) in relation to the nearby central volcanoes (polygenetic volcanoes), namely Hekla, Hengill, Eyjafjallajökull, and Katla. Also shown are the nearby volcanic systems. The main N-striking dextral parts of the June 2000 earthquakes, where a denotes the 21 June rupture and b denotes the 17 June rupture, are indicated. The horizontal arrows indicate the general sinistral movement across the SISZ. Modified from Gudmundsson and Brenner (2003).

during which the largest shocks may reach magnitude 7.1 and possibly 7.2 or 7.3 (Stefansson et al., 1993; Stefansson et al., 2000; Einarsson, 2008). Prior to the M6.6 earthquakes in June 2000 (Stefansson et al., 2000; Bergerat and Angelier, 2001; Angelier and Bergerat, 2002; Pedersen et al., 2003) the last such sequence was in 1896. There was also a single, instrumentally determined earthquake of magnitude 7 in 1912 in the easternmost part of the SISZ (Bjarnason et al., 1993; Belardinelli et al., 2000; Stefansson et al., 2000) and a M6.3 earthquake in the westernmost part of the SISZ in 2008 (Sigbjörnsson et al., 2009; Hench et al., 2016; Arnardottir et al., 2018).

The surface of the SISZ is partly covered with Holocene basaltic lava flows, and partly with Pleistocene rocks. The faults that dissect the Holocene lava flows are most easily traced, but these lava flows cover areas of relatively narrow north-south extent. Over periods of years and decades, the microseismicity of the SISZ is mostly confined to about 70 km long (E-W) and 10-20 km wide (N-S) zone (Rognvaldsson, 1994; Bergerat et al., 1998; Bergerat and Angelier, 2001; Parameswaran et al., 2020, 2023). Strike-slip faults giving rise to earthquakes of magnitude 7.1, however, are commonly 40-80 km long (Wells and Coppersmith, 1994; Ambraseys and Jackson, 1998). Gudmundsson (1995a) therefore suggested that the fault arrays associated with the largest earthquakes may reach lengths of tens of kilometres and that the N-

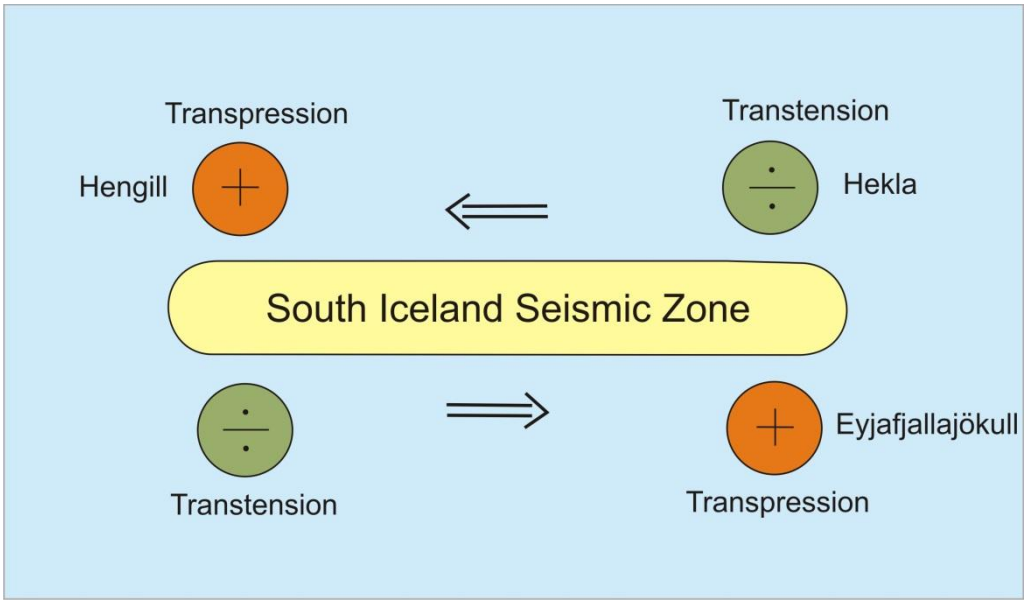

Fig. 3. During normal sinistral displacement across the SISZ, Hekla concentrates relative tensile stresses (is in a quadrant of transtension), whereas Hengill and Eyjafjallajökull concentrate relative compressive stresses (are in a quadrants of transpression). Thus, these volcanoes are subject to compressive stresses that may generate doming (uplift) and earthquakes with or without magma intrusion. In the case of dike injection, there would be a strong tendency for dikes to become arrested, and some to be deflected into sills, at contacts between mechanically dissimilar layers inside the volcanoes. These scenarios were, indeed, observed in Hengill and Eyjafjallajökull prior to the June 2000 earthquakes.

S width of the South Iceland Seismic Zone may be as large as 60 km. This proposal has been supported by later studies (Luxley et al., 1997; Passerini et al 1997; Bergerat et al., 1998; Gudmundsson, 2017). Furthermore, an analysis of one of the main NNE-trending faults in the SISZ, the Holocene Leirubakki Fault, indicates a surface rupture length of around 50 km (Bergerat et al., 2002). In the numerical models below, we therefore test the effects of 45-60-km-long northerly-striking dextral faults on the local stresses around Eyjafjallajökull and Katla.

The Holocene and Pleistocene parts of the SISZ both display seismogenic faults consisting of conjugate arrays of fractures trending NNE and ENE (Gudmundsson, 1995a; Bergerat et al., 1998; Bergerat et al., 2003; Parameswaran et al., 2020, 2023). These conjugate systems have also been confirmed by the fracture pattern generated during the M6.6 June 2000 earthquakes (Bergerat and Angelier, 2001; Angelier and Bergerat, 2002; Clifton and Einarsson, 2005; Gudmundsson, 2017).

3. Deformation in Hengill and Hekla

3.1 Hengill

The Hengill Central Volcano (Figs. 2-4), a part of a volcanic system of the same name (Fig. 1), has not eruped since since 2000 BP. The Hengill area is sometimes divided in two central volcanoes, Hengill and Hrodmundartindur (east of Hengill). Because, the eruptive material in Hrodmundartindur is identical in composition to that erupted in Hengill (A.T. Gudmundsson 2001) they are here regarded as one and the same central volcano, referred to as Hengill.

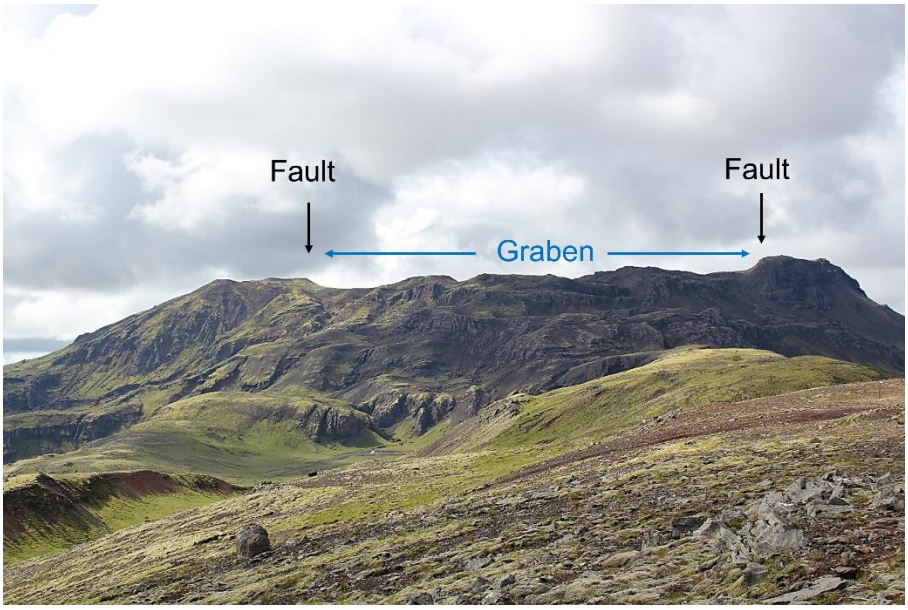

Fig. 4. View southwest, the Hengill volcano is composed mainly of hyaloclastites, lava flows, and intrusions - very similar in structure to Eyjafjallajökull (Fig. 7). The top part of Hengill is dissected by major normal faults that form a graben.

The Hengill Volcano is mostly composed of basaltic hyaloclastites, pillow lavas, and pillow breccias, but it contains also intermediate (andesitic) and acid rocks (Saemundsson 1996; Gudmundsson, 2017). The peak of Hengill is at 803 m.a.s.l and its estimated age is 0.8 Ma. It is a rift-zone central volcano with many large normal faults and grabens (Fig. 4; Gudmundsson, 2017; Steigerwald et al., 2020), some exceeding 200 m in vertical displacement, but no collapse caldera. Although Hengill has, as yet, no collapse caldera, it is likely to have an active shallow magma chamber. This conclusion follows from the intense hydrothermal activity in Hengill, its acid and intermediate rocks, and the high number of inclined sheets which, according to drill-hole data, in places make up about 50% of the rock at 1.5 km depth and nearly 100% of the rock below 2 km depth (Saemundsson 1996).

Hengill and its surroundings were subject to an accelerated crustal deformation from 1994 to 2000. The deformation began in July 1994 with a swarm of moderate-size earthquakes (Sigmundsson et al., 1997; Rognvaldsson et al., 1998; Feigl et al., 2000). Part of the deformation and seismicity occurred southeast of the Hengill Volcano, and part along an ENE-trending zone, 14 km long and 2-3 km wide (N-S), located south of Hengill (Rognvaldsson et al., 1998; Parameswaran et al., 2020, 2023). In fact, the centre of the uplift episode was 6-7 km southeast of the top of the Hengill Volcano (Ducrocq et al., 2021). The largest ($M > 4$) earthquakes in this swarm, as in the earlier activity from 1994 in Hengill and its surroundings, are thought to be associated with N-trending, dextral faults (Rognvaldsson et al., 1998). Many earthquakes in Hengill, particularly in its southeastern part and further to the south, are also likely to be associated with ENE-trending sininstral faults, that is, conjugate faults to the N-trending dextral faults (Parameswaran et al., 2020, 2023).

The deformation in and around Hengill was primarily uplift, crustal doming, with a maximum uplift rate of 2 cm/year. This doming may be partly related to magma intrusion at around 7 km depth (Feigl et al., 2000). Since the inferred centre of the uplift is 6-7 km southeast of the top of Hengill it follows that the uplift cannot be explained in terms of expansion of the inferred Hengill magma chamber on receiving new inflow of magma. And even if one would regard Hrodmundartindur as an independent central volcano, it is located directly east of Hengill itself (e.g. Steigerwald et al., 2018) and thus an expansion of any potential (but unconfirmed) magma chamber of Hrodmundartindur would not fit at all with the centre of uplift. There is in fact no active central volcano at the location of the centre of uplift. A sill, injected lateral to the southeast from Hengill, might be a source, but we know of no evidence indicating such a lateral sill propagation during the 1993-1999 inflation.

Part of the deformation is likely to be related to Hengill being located in an area of transpression and thus to compressive stress transfer from the SISZ (Figs. 1-3; Gudmundsson and Brenner, 2003). Hengill and its magma chamber function as an elastic inclusion that concentrates stresses, in this case the compressional stresses transferred to the volcano during loading of the SISZ. All active volcanoes with magma chambers functions as elastic inclusions and concentrate stresses - as is well demonstrated by simple numerical models (Andrew and Gudmundsson, 2008).

3.2 Hekla

Hekla is an elongated volcano (Fig. 5), a volcanic ridge, that reaches an elevation of 1480 m a.s.l. and has a clear 5.5-km-long summit fissure, the Hekla Fissure, where most of the proper Hekla eruptions take place (Fig. 5). The adjacent tectonic fractures and volcanic fissures strike mostly N40-45°E; by contrast Hekla itself strikes N65°E, which coincides with the general trend of the sinistral faults of the SISZ, suggesting that the summit fissure of Hekla was initially an ENE-trending sinistral fault of the SISZ (Gudmundsson et al. 1992; Gudmundsson and Brenner, 2003). In that model, accumulation of tensile, and partly shear, stresses in the transtension quadrant where Hekla is located (Figs. 1-3) contributes to the frequent rupturing and associated eruptions of Hekla through a multiple dike (Gudmundsson, 2025c).

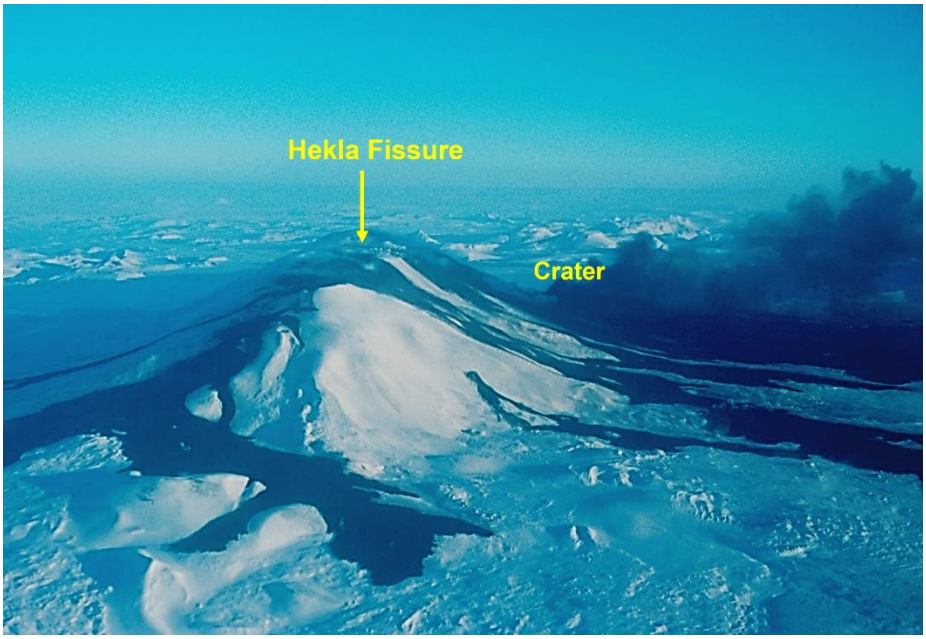

Fig. 5. View north, an aerial photograph of the Hekla volcano as seen in January 1991 during an eruption. The black spots are the newly erupted lava flows. The entire volcano is a ridge dissected by the Hekla Fissure (Heklugja). The active crater is seen in the upper right part of the photograph (cf. Gudmundsson et al., 1992).

In terms of frequency of eruptions, as well as production of lava and tephra, Hekla is one of the most active central volcanoes in Iceland. During the past 1100 years since the settlement in Iceland (historical time), there have been at least 18 eruptions in Hekla itself, and 4-5 in its immediate vicinity (Gudmundsson et al., 1992; Thordarson and Larsen, 2007; Thordarson and Höskuldsson, 2014), the most recent one being the February 2000 eruption. Hekla forms the central part of the Hekla Volcanic System. This system is variously estimated as 40 km long and 7 km wide (Jakobsson 1979) or as 60 km long and 19 km wide (Thordarson and Höskuldsson, 2008, 2014). During the Holocene, the Hekla System has produced basalts, basaltic andesites, andesites, and dacites-rhyolites.

Jakobsson (1979) suggests that all the andesites and acid rocks produced during the Holocene were erupted from the Hekla Fissure, and that all the basaltic andesites erupted within 9 km of Heklugja. At greater distances from the Hekla Fissure, out to the northeast and southwest margins of the Hekla System, only basalts have been erupted. Gudmundsson et al. (1992) propose that Hekla is fed by a density-stratified magma chamber. The depth to the proposed density-stratified magma chamber beneath Hekla is, however, not well constrained; estimates vary between 5 km and 24 km (Geirsson et al., 2012).

In historical time, the repose period of Hekla has been from 9 to 120 years. The shortest one so far is the repose period preceding the February 2000 eruption, 9 years; the repose periods prior to the 1980, 1991 and 2000 eruptions have also been unusually short. The unusually short repose periods prior to the most recent eruptions may be partly related to tensile (and shear) stress concentrations around Hekla in response to loading of the SISZ to failure (Fig. 6). In terms of this model (Gudmundsson and Brenner 2003) the unusually high frequency of eruptions in Hekla in two decades prior to the June 2000 earthquakes is partly due to its being located in an area of transtension at one end of the SISZ (Figs. 1-3, 6) at the time when much tensile stress had accumulated (concentrated) in and around Hekla. In this model, loading of the SISZ and associated tensile stresses in the Hekla area are likely to trigger frequent eruptions in Hekla primarily if the summit fissure (and its extension to the source magma chamber) is already occupied by a dike-injection (as a part of an existing multiple dike, Gudmundsson, 2025c) that is not completely solidified, and thus with a low tensile strength. Such a dike-injection was provided by the 1970 Hekla eruption. Thus, in this model, frequent low-volume eruptions of Hekla are likely to occur if, by chance, an eruption, such as the one in 1970, occurs just prior to the last decades of the seismic cycle that leads to major earthquakes in the SISZ.

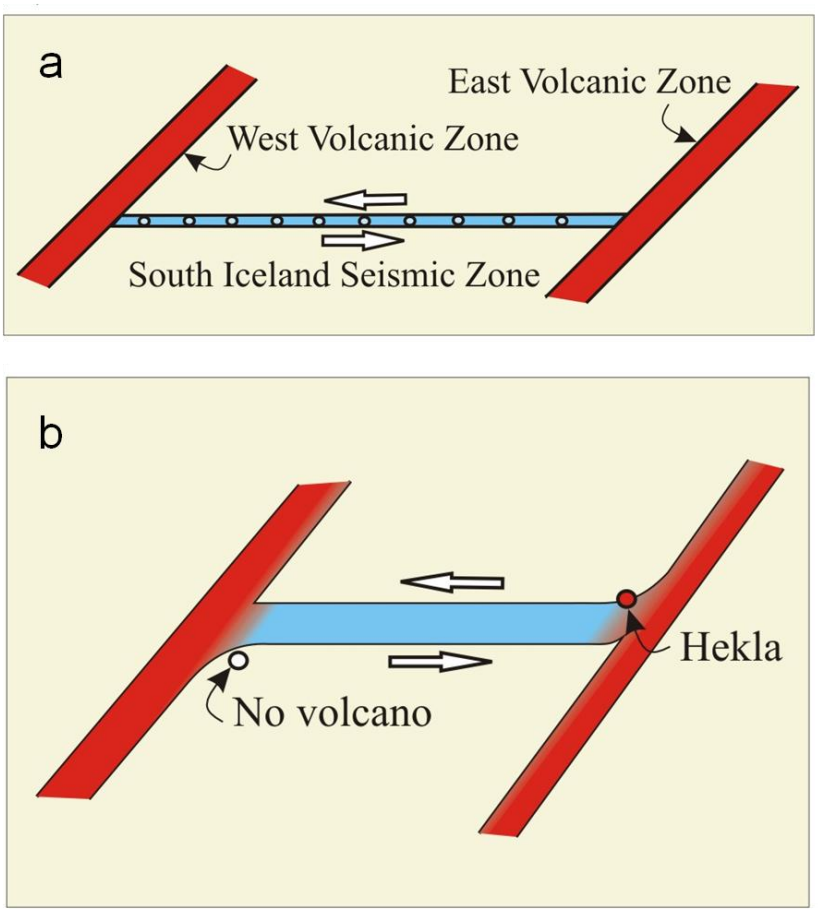

Fig. 6. The overall movement across the SISZ is sinistral, which results in transtension and transpression in the various quadrants at the ends of the SISZ (cf. Fig. 2). One reason for the frequent eruptions from the Hekla volcano in 1970-2000 is the tensile stress that had concentrated in and around the volcano due to stress transfer from the SISZ. No volcano is located in the other quadrant of transtension.

4. Eyjafjallajökull

4.1 The volcano

A stratovolcano (Figs. 3, 7a) reaching 1666 m a.s.l., Eyafjallajökull has an east-west strike, being about 30 km long (east-west) and 8 -14 km wide (north-south). There is a small collapse caldera at its top, about 2.5 km in diameter. The volcano is composed of rocks that have piled up during the past 0.8 Ma, but it has shown little activity during Holocene. It is mainly composed of hyaloclastites (basaltic breccias) and lava flows, but has also numerous intrusions, in particular dikes and sills (Fig. 7b; Thordarson and Höskuldsson, 2014; Gudmundsson, 2017).

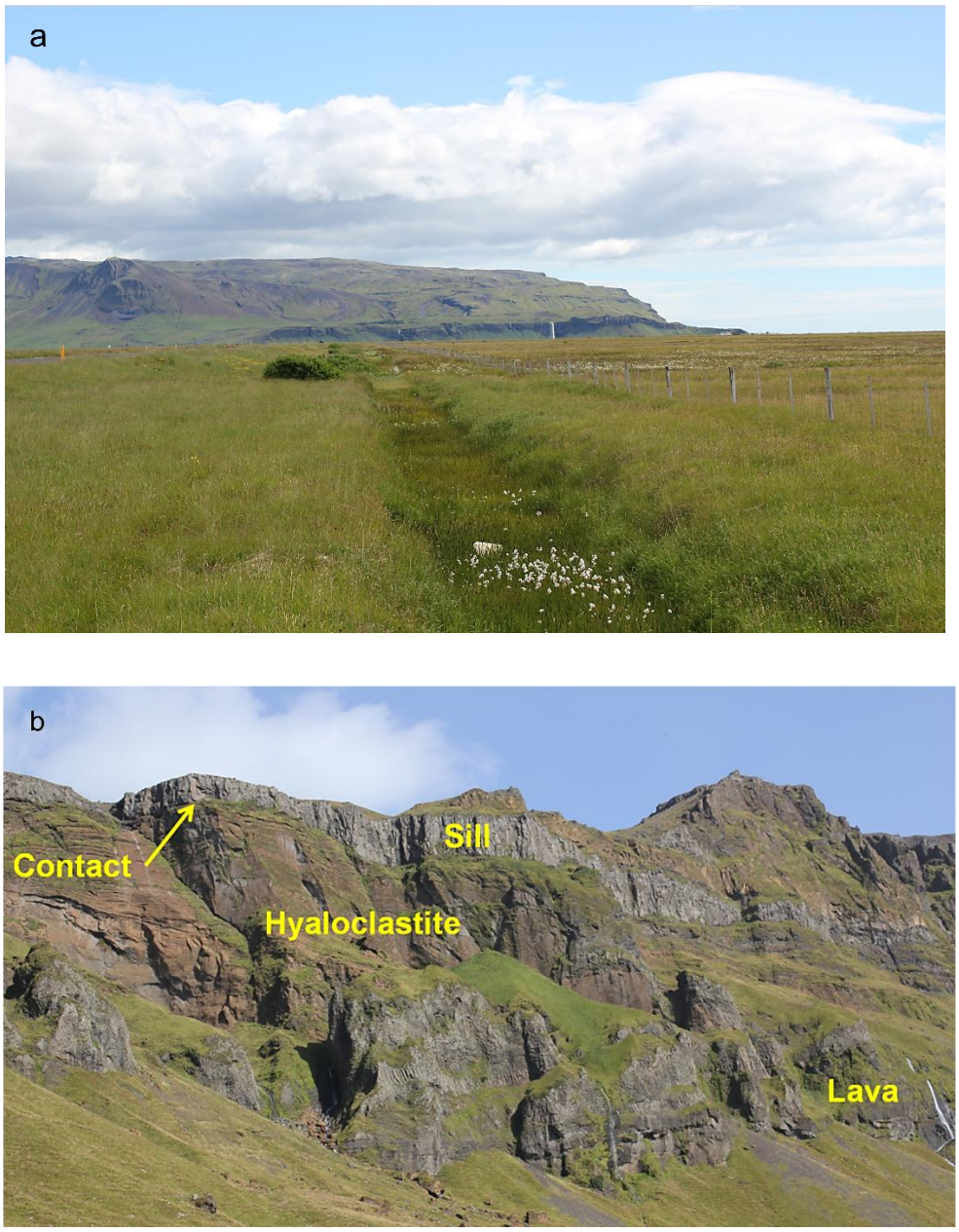

Fig. 7. Eyjafjallajökull volcano. a) View east, the southern part of the volcano, the waterfall being Seljalandsfoss. b) View north, showing a close-up of part of the southern flanks of Eyjafjallajökull with its complex internal structure, including hyaloclastites, lava flows, and sills (Gudmundsson, 2017).

Prior to the 2010 eruptions, there were at least two eruptions - and possibly four - in the volcano in historical time (the past 1100 years). One is well documented and happened in December 1821. This eruption was from the caldera in the top of the volcano, just like the second of the 2010 eruptions. The was apparently little or no eruptive activity in the early part of 1822 and then in June 1822 the eruption became much more powerful with ash reaching all the way west to the capital Reykjavik. This eruption was thus discontinuous, and may be regarded as two eruptions with a total (intermittent) duration of about 15 months. Less well-documented eruptions occurred in AD 920 and 1612 or 1613 (Sigmundsson et al., 2010).

4.2 The 2010 eruptions

The 2010 eruptions are described in detail by Sigmundsson et al. (2010), Gudmundsson et al. (2012), Karlsdottir et al. (2012), and Thordarson and Höskuldsson (2014), and its specific aspects in many other reports and papers, so that only a brief description of the events is given here. An effusive fissure eruption began 20 March 2010 in the pass between the glaciers Eyjafjallajökull and Myrdalsjökull, referred to as Fimmvörduhals. This flank eruption, producing low-viscosity primitive basalt, came to an end 12 April. The fissure had a clear north-northeast trend, was about 500 m long (Gudmundsson et al., 2012) and with a maximum opening of 1-1.5 m (Sigmundsson et al., 2010). This would give an aspect (length/opening) ratio for the volcanic fissure/feeder-dike at the surface of about 500, in good agreement with data from other feeder-dikes in Iceland and elsewhere (Galindo and Gudmundsson, 2012; Kusumoto et al., 2013; Hobe et al., 2025).

A second eruption began 14 April in the summit caldera. This eruption was subglacial, highly explosive and produced ash of an intermediate (trachyandesitic) composition (Gislason et al., 2011). The magma supplied during the eruption came from a shallow magma chamber, at about 4-5 km depth (Karlsdottir et al., 2012; Tarasewicz et al., 2012), which is associated with the summit collapse caldera. The eruption column reached a maximum altitude of about 11 km, and the resulting ash clouds had major disrupting effects on air traffic in Europe for many days. The eruption came to an end on 22 May 2010. There were three fissures associated with this eruption, all of them several hundred metres long (maximum 6-700 m). Two of the fissures strike north-north east; one is inside the caldera, the other is outside the caldera. The third fissure, which produced most of the eruptive material, has an east-west strike (Gudmundsson et al., 2012). These three fissures thus reflect the main tectonic trends in Eyjafjallajökull, namely the east-west trend, which is the main trend of the volcano itself and the associated system, and the northeast trend which is the general trend of the East Volcanic Zone and its propagating off-rift extension - namely the part which contains Eyjafjallajökull and Katla (Fig. 1).

Both eruptions in Eyjafjallajökull were very small. The earlier effusive fissure eruption produced about 0.02 km^3 and the later explosive eruption produced an ash volume with a rock-equivalent volume of about 0.18 km^3 (Gudmundsson et al., 2012). Thus, the total volume of solid rock produced in these two eruptions is about 0.2 km^3, similar to typical small eruptions in the central volcanoes of Iceland (Gudmundsson, 1995b; Thordarson and Larsen, 2007; Thordarson and Hoskuldsson, 2008).

4.3 Earthquakes and deformation

As indicated above, there were episodes of crustal deformation in Eyjafjallajökull prior to the 2010 eruptions. Before the introduction of a dense seismic network (the South Iceland Lowland, SIL, network) in the late 1980's and early 1990's, no earthquakes had been recorded in or beneath Eyjafjallajökull (Jakobsdottir, 2008). In the years 1991-1993 some 70 small earthquakes (M2.5 or less) were recorded in the volcano. These were followed by earthquake swarms which occurred in Eyjafjallajökull in 1994-1995, in 1996, in 1998, in 1999, and in the spring (until the end of May) of 2000. The largest earthquake associated with this activity reached M3.6 in March 1999 (Jakobsdottir, 2008). From mid-2000 until mid-2009, there were few earthquakes and negligible deformation in Eyjafjallajökull (Sigmundsson et al., 2010), that is, following the two M6.6 earthquakes in the SISZ.

There was crustal deformation associated with the seismic activity in Eyjafjallajökull, in particular two main periods of uplift (Jakobsdottir, 2008; Sigumundsson et al., 2010). The first main uplift period was from September 1993 to September 1994, the second from July to August 1999. The main uplift was apparently associated with the 1999 episode, reaching a maximum uplift of about 0.35 m at a distance of about 4 km south of the summit (Sturkell et al., 2010). Using homogeneous, elastic half-space models, these uplifts have been interpreted as being related to the emplacement of two sills at roughly 4.5-6.5 km depth below the surface of Eyjafjallajökull (Sigmundsson et al., 2010).

Many conceptual interpretations of these inferred sill-emplacement episodes have been suggested. For example, Sturkell et al. (2010) in their conceptual model of the two sills show them at depths of about 3.8 km and 5.2 km, respectively. Similarly, in their conceptual model of the sills Sigmundsson et al. (2010) show the sills at depths of about 5.5 km and 6.1 km. Also, Tarasewicz et al. (2012) show many sills, at depths of as much as 24 km, which apparently were emplaced shortly before the 2010 eruptions and supplied magma to the eruptions.

The lateral dimensions of the sills, as indicated by the conceptual models, also vary considerably. Thus, Sturkell et al. (2010) show both the sills in an east-west cross section with the same lateral dimension (diameter or strike dimension), namely as about 10 km. By contrast, Sigmundsson et al. (2010), again in an east-west cross section, show the 1994 (upper) sill with a lateral dimension of about 17 km, and the 1999 (lower) sill with a lateral dimension of about 11 km. These are clearly meant to be schematic illustrations. However, since they are based on basically the same data, the variation in dimensions and location of the inferred sills indicates the difficulty in obtaining accurate location and sizes of the sills, that is, the depth and geometry of three-dimensional structures from essentially two-dimensional deformation data.

More intensive earthquakes and deformation in Eyjafjallajökull started again in around mid-2009 for some weeks, and then again from December 2009, with several earthquakes per day (Sigmundsson et al., 2010). The rate of deformation increased significantly after 4 March until an eruption began on 20 March 2010. During the effusive eruption itself (20 March - 12 April) there was effectively no deformation detected. During the summit eruption, from 14 April to 22 May, there was slow deflation of the summit.

These deformation episodes have also been interpreted in terms of sill inflation and deflation. The model scenario proposed by Sigmundsson et al. (2010) is briefly as follows. From December 2009 to February 2010, a sill inflated at a depth of 4-5.9 km (their sill 1) under the southeastern flank of the volcano. From the beginning of March until the 20 March (beginning of the effusive eruption) a second sill inflated at the same depth, but under the northeastern flank of the volcano. At the same time, an inclined ENE-striking dike formed, presumably extending from sills to within a few hundred metres of the surface. This dike must have rotated on reaching closer to the surface, since there it supplies magma to a NNE-striking fissure (the main fissure; a small NW-trending offshoot from that fissure was formed 31 March). The deflation of the summit, associated with the explosive eruption from 14 March to 22 May, is related to a third sill which has depth estimates from 3 km to 4.7 km.

A more complex interpretation is offered by Tarasewicz et al. (2012). They suggest that in addition to a shallow sill-like magma chamber at about 5 km depth beneath the summit caldera - and supplying magma to the second, that is, the explosive eruption - there were at least 4 sills formed during or just prior to the two 2010 eruptions. The main feeder-dike for the effusive eruption is, in this model, the same as the one that triggered the explosive eruption, and this dike meets with all the sills - and apparently receives magma from them - on its way to the surface. The stress conditions that would favour the formation of all these sills at very different depths (about 5 km, 12 km, 20 km, and 24 km) over a short time and allow the feeder-dike to meet all the sills and still continue to the surface are not explored, but would be needed in a further quantitative elaboration of the model.

Clearly, the models proposed above to explain the deformation in Eyjafjallajökull in the decades prior to the 2010 eruptions, as well as during the eruption, are complex. They are also strikingly different, given that they are supposedly all based on the same data from an exceptionally well-monitored volcano. Part of the complexity may be related to the fact that all the models assume homogeneous and isotropic rock properties for the Eyjafjallajökull and the associated crustal segment, whereas the volcano is known to be exceptionally heterogeneous and highly anisotropic as regards its exposed parts (Fig. 7b). Stress rotation, delamination, and

elastic-mismatch effects are known to affect dike and sill paths and the probability of dikes deflecting into sills at contacts between mechanically dissimilar layers (Gudmundsson, 2011, 2022). Thus, for a further analysis of the deformation data as regards dikes and sills, considerations of the mechanical layering of the crustal segment on the intrusion paths would no doubt be very useful.

5. Katla

5.1 The volcano

Katla is a collapse caldera. The caldera itself is about 100 km^2 and elongated in a northwest-southeast direction. Katla forms the southernmost part of a volcanic system of the same name (Figs. 1, 2), which has a northeast length of 90-110 km and a width of about 30 km (Thordarson and Larsen, 2007; Thordarson and Höskuldsson, 2008, 2014). The caldera is covered by the Myrdalsjökull ice cap, with a summit elevation of about 1512 m a.s.l. Geophysical studies indicate that the caldera is as deep as 600-750 m. Beneath the caldera there is a shallow magma chamber with a top at about 1.7 km depth (Sturkell et al., 2010).

Katla has erupted frequently in the past 1100 years and is generally regarded the most productive volcanic system in Iceland in historical time in terms of volume (a total of 25 km^3 calculated as solid eruptive materials) and, with 21 known eruptions, the third most active in terms of eruption frequency (Thordarson and Larsen, 2007). It produces mostly FeTi basalts that are mostly erupted within the main caldera. The volcano Katla has been active for at least 0.2 Ma.

The last well-documented eruption occurred in 1918, with an estimated solid-rock volume of about 1 km^3 (Sturkell et al., 2010). There are some indications of a small subglacial eruption in 1955, and possibly also in 1999 and 2011, but not eruptive materials were observed in any of these events and they must all be regarded as unconfirmed. Thus, the most recent well-documented and large eruption is still the 1918 eruption. The largest historical eruption in the Katla Volcanic System, however, occurred outside the caldera, namely the 934-938 AD eruption of Eldgja (Thordarson and Larsen, 2007). This eruption occurred on a 75-km-long segmented volcanic fissure, partly located in a graben, and produced a total of about 20 km^3 of lava and tephra. This makes the Eldgja eruption the largest one in Iceland in historical time.

5.2 Earthquakes and deformation

Earthqukaes and deformation occur primarily at two locations in the Katla area: one is inside the caldera itself, the other is in the western part of the Myrdalsjökull ice cap (a place

called Godabunga), close to the pass between Katla and Eyjafjallajökull (Fig. 2; Jakobsdottir, 2008; Sturkell et al., 2010). The Godabunga earthquakes, mostly at about 1.5 km depth (Sturkell et al., 2010), are much more frequent and show seasonal variations, being most common in the second half of each year. It has been suggested that the Godabunga earthquakes are partly of non-tectonic origin or, alternatively, that they may be related to changes in pore-fluid pressure associated with melting of the ice cap, while other interpretations (such as cryptodome intrusion) have also been proposed (Sturkell et al., 2010). The earthquakes inside the Katla caldera, however, are of tectonic origin (Jakobsdottir, 2008; Sturkell et al., 2010).

GPS measurements indicated uplift of one point, located on the northeast rim of the Katla caldera, from 2000 to 2004, but similar changes were not seen in InSAR measurements of the flanks of the volcano (Sturkell et al., 2010). It has been suggested that part of this uplift may be related to a magma intrusion, possibly at 2-5 km depth (Sturkell et al., 2010). However, the data is clearly too inaccurate to make any reliable estimates of a possible magma source. Since 2004 the main deformation of Katla can be attributed to gradual thinning of the Myrdalsjokull ice cap (Sturkell et al., 2010).

6. Local stresses in Eyjafjallajökull and Katla

6.1 Background

The general loading of the SISZ puts Eyjafjallajökull (and, to a lesser degree, Katla) in a quadrant of compression - transpression (Figs. 1-3). This is confirmed by earlier numerical models which show that local compressive stresses around Eyjafjallajökull reach as much as 17 MPa (Fig. 8a; Gudmundsson and Brenner, 2003).

We have made new numerical models, using the finite element program Abaqus (Smith, 2009), showing the effects of loading from the SISZ on the local stresses around both Eyjafjallajökull and Katla. The volcanoes are modelled as holes, either empty or filled with magma under excess pressure. This model is clearly suitable for Katla, partly because Katla is a collapse caldera with a shallow magma chamber (Sturkell et al., 2010). Additionally, Katla is primarily made of hyaloclastites and thus acts as a soft inclusion (Andrew and Gudmundsson, 2008). The situation in Eyjafjallajökull is more complex. Our geometry of the volcano reflects the east-west elongated shape of the volcano itself. Since it is primarily made of soft hyaloclastites (with many intrusions and lava flows, however), the volcano, like Katla, acts as a soft inclusion. As indicated above, some interpretations suggest that there may have been partially molten sills in the volcano emplaced in the decade before the June 2000 earthquakes. In particular, the sill supposed to have been emplaced during the 1994 unrest is very large -

with a diameter of as much as 17 km (Sigmundsson et al., 2010) - and acting as an elongated hole in the volcano. Such a sill would further justify the modelling of the volcano as an elongated hole or a soft inclusion. We use a dynamic Young's modulus between 80 GPa and 130 GPa for the crust in South Iceland. The lower value applies to the upper part of the crust, where the magma chambers are located, that is the depth from about 1.5 to 9 km, whereas the higher value applies to the crustal layer below about 9 km depth (Gudmundsson, 1988). For calculating the effects of stress transfer from the SISZ, we use the lower value, 80 GPa, but the higher values for some models on the effects of N-S strike-slip faulting on the local stresses. This is because the faults extend to depths of 14 km or more in the eastern part of the SISZ (Rognvaldsson, 1994). A Poisson's ratio of 0.25 is used for all the crustal layers (Gudmundsson, 2011). For the general stress transfer from the SISZ to the volcanoes, we use a compressive horizontal loading of 10 MPa. This is loading is in accordance with likely values based on geological and seismological studies in South Iceland (Stefansson et al., 1993; Gudmundsson and Brenner, 2003; Angelier et al., 2004a,b).

The results show that high compressive stresses concentrate around the volcanoes and thus agree with the earlier model (Fig. 8a). In addition there are tensile stresses at the lateral east-west ends of the volcanoes, and in particular in the narrow zone between the volcanoes. For the given general stress field associated with stress transfer from the SISZ, the horizontal compressive stresses inside the volcanoes would tend to be magnified in the stiff (high-Young's modulus) layers and units. This follows because, in a layered crust, stiff layers take up more of the loading (compressive or tensile) than soft layers, so that, during compression, the stiff layers may become subject to high compressive stresses (Gudmundsson, 2011). This means that the maximum principal compressive stress σ_1 would tend to be horizontal inside the volcanoes as well as within crustal segments to which they belong. The high horizontal compressive stresses would encourage the deflection of dikes into sills at contacts between mechanically dissimilar layers (Gudmundsson, 2011), particularly at the contacts between soft hyaloclastites and stiff lava flows or earlier sills (Fig. 7b). Thus, the tendency for dikes to change into sills - that is, for the dikes to become arrested, at least temporarily - is particularly strong in Eyjafjallajökull because of the contrasting mechanical properties of the rocks that constitute the volcano.

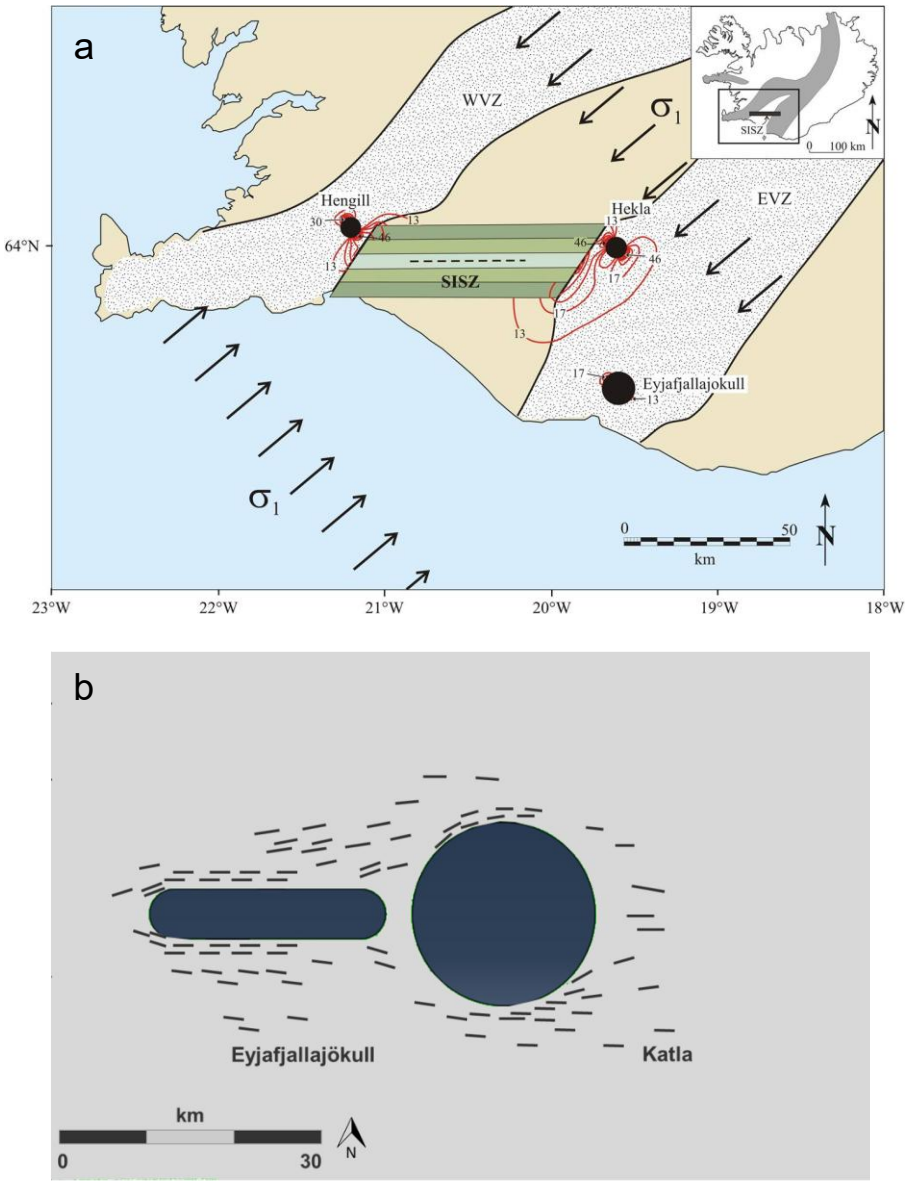

Fig. 8. Schematic illustration of the compressive stresses in nearby volcanoes during normal sinistral movement across the SISZ and the associated stress transfer. a) With normal maximum horizontal compressive stress (σ_1) acting in a NE-SW direction (based on earthquake data) in South Iceland, compressive stresses tend to concentrate at Hengill and Eyjafjallajökull. Here σ_1 = 10 MPa, which generates local compressive stresses of up to 30 MPa in Hengill and 17 MPa in Eyjafjallajökull (modified from Gudmundsson and Brenner, 2003). b) If a simple model of a 10 MPa east-west compression is used, with a very schematic presentation of Eyjafjallajökull and Katla, the maximum principal compressive stress ticks (trajectories) might trend similar to what is indicated here. Eruptions are generally not favoured, and those that might occur would be on roughly east-west striking dikes.

6.2 Effects of fault slip on the local stresses: short faults

The eruptions in Eyjafjallajökull took place after the 2000 earthquakes in the SISZ, whereas for the decade prior to the earthquakes there is evidence that there were magma injections into the volcano which, however, were unable to reach the surface of the volcano. Clearly, the two earthquakes modified the stress field that had been building up for decades in the SISZ and the surrounding volcanoes (Figs. 1-7). Stress changes following earthquakes diminish with distance

from the slipping fault. Since the fault that ruptured on 17 June 2000 is closer to Eyjafjallajökull than the one that ruptured on 21 June 2000, we focus mainly on the former when modelling the stress effects of the fault slip on Eyjafjallajökull and Katla.

The main earthquake faults, based on the surface ruptures, of the June 2000 earthquakes were about 20-25 km long, in a north-south direction (e.g., Bergerat and Angelier, 2003). Inverse modelling using dislocations indicate that the displacements could be explained by strike-slip faults with lengths of about 15 km in a north-south direction (Arnadottir et al., 2008; Einarsson, 2008). Aftershock locations indicate fault lengths of 12.5 km (June 17 fault) and 16.5 (June 21 fault) km, the faults being highly segmented, with some of the segment showing clear sinistral movements and reaching lengths of 2-3 km (Hjaltadottir and Vogfjord, 2005). Thus the faults form conjugate strike-slip faults, the main dextral segments striking due north and the sinistral segments striking due east-southeast (Hjaltadottir and Vogfjord, 2005). These seismological results are confirmed by direct surface observations of the faults - which show numerous conjugate segments in South Iceland (Gudmundsson, 1995a; 2017Bergerat and Angelier, 2003; Clifton and Einarsson, 2005). The maximum depth of both earthquakes, that is, the thickness of the seismogenic layer is modelled as 10 km and the maximum subsurface displacements as 2.6-2.9 m (Pedersen et al., 2003).

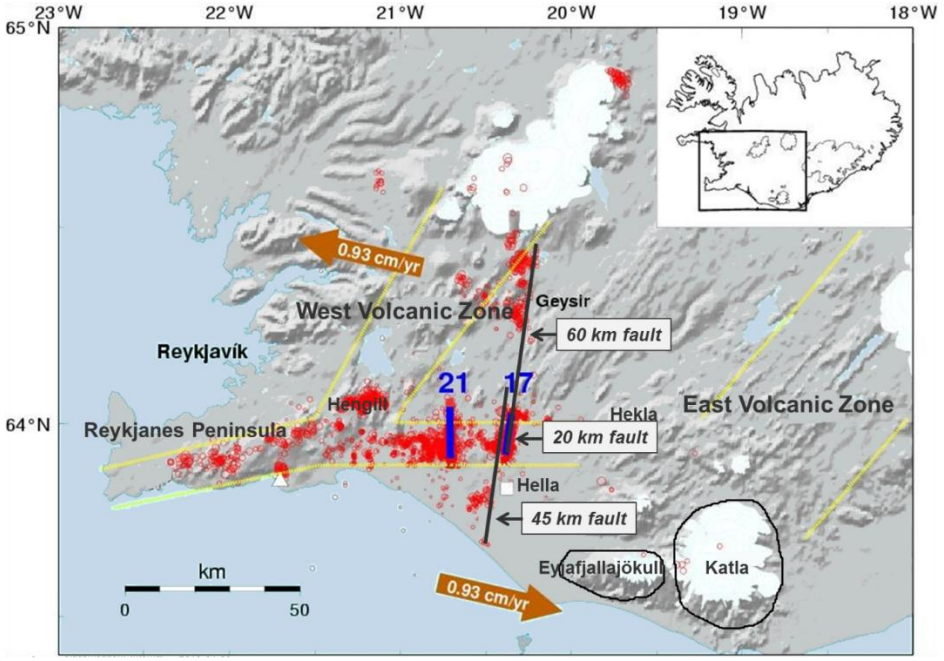

Fig. 9. Map showing the location (blue thick lines) of the June 17 (Arnes Fault) and June 21 (Hestfjall Fault) earthquakes in 2000 and the associated triggered earthquakes (from Stefansson et al., 2003). These faults are used for the basis of the modelling in Fig. 10. Also indicated are the spreading vectors and rates and the volcanoes Hengill, Hekla, Eyjafjallajökull, and Katla in relation to those earthquakes. Added to these are potential future earthquake faults; a 60 km long fault extending north to Geysir and a 45 km long fault extending south to the coast. These are hypothetical locations but both originate in the microseismic part of the SISZ and the fault lengths are to be expected in earthquakes reaching M7.1 or more. These hypothetical seismogenic faults are used as a basis for the modelling in Fig. 11.

All faults are segmented, so that it is commonly difficult to decide on the exact length (strike dimension) or height or width (dip dimension) of a fault. In the June 2000 earthquakes, for example, there were earthquakes continuing far south and north of the main rupture areas (Fig. 9). These earthquakes, particularly in the Geysir area, were triggered by the stress changes associated with the main shocks (Hjaltadottir and Vogfjord, 2005; Jakobsdottir, 2008). Some of the reactivated faults in the Geysir area strike northeast and dip 76° and may be reactivated normal faults. But there are also conjugate faults in the Geysir area, of the type found further south, that were reactivated during the June 2000 earthquakes and for some time following those earthquakes (Thorbjarnardottir et al., 2018). These are primarily NNE-striking dextral faults, are close to vertical, and up to at least 6 km in length (strike dimension), while some may be longer. Then there are ENE-striking sinistral faults, also close to vertical and up to 2.5 km in length (strike dimension). Similarly, the northernmost segment of the fault of 21 June (Hestfjall) dips 77°, but due north (Hjaltadottir and Vogfjord, 2005), indicating that it is a mixed-mode fault, partly strike-slip and partly dip slip. Clearly, the faulting associated with the June 2000 earthquakes was complex (as seismogenic faulting normally is), involving many segments of different strikes and dips and with a different sense of slip. Nevertheless, to get a general idea of the effect of faulting on the stresses around the nearby volcanoes, Eyjafjallajökull and Katla, some simple numerical models may be of help.

We first have to decide on the attitude and length of the modelled faults. We have seen that the length estimates for the June 2000 faults vary from 12.5 km to 25 km or by 100%. This is understandable since the faults are segmented and it is partly a matter of definition which segments are regarded as belonging together during the earthquake. Also, some surface ruptures may be related to the stresses associated with the passing of the seismic waves rather than the fault rupture itself. Again, in many cases it is a matter of definition or convention whether such segments were regarded as part of the earthquake rupture or as 'secondary' structures. Here we model the faults as 20 km long. The length is roughly the 'average' of most estimates. As in the stress models above, we use a typical Poisson's ratio of 0.25 and a dynamic Young's modulus between 80 GPa and 130 GPa for the crust. It should be noted that the fault slip is largely determined by the stiffest part of the crustal segment hosting the fault. The 2000 earthquakes originated at depth of about 5-6 km (earthquake foci; Bergerat and Angelier, 2003) but they ruptured the entire seismogenic layer, down to depths of 10 km or more (Hjaltadottir and Vogfjord, 2005). At the depth of 9-10 km, the dynamic Young's modulus is about 130 GPa, whereas at 4-9 km it is around 80 GPa (Gudmundsson, 1988).

We use two types of loading: displacement loading and stress loading. The displacement loading is based on the inferred displacement during faulting. For example, the maximum displacement of the June 2000 faults is estimated at about 2.9 m (Pedersen et al., 2003). For a 3 m displacement, or 1.5 m on each side of the strike-slip fault, the stress changes can be calculated; in particular those that occur in the nearby volcanoes. Similarly, the stress drop (driving shear stress) in most earthquakes is normally in the range of 0.1-10 MPa, the overall general range being around 0.03-30 MPa (Kanamori and Anderson, 1975; Scholz, 2002). Here we use 10 MPa as the driving shear stress.

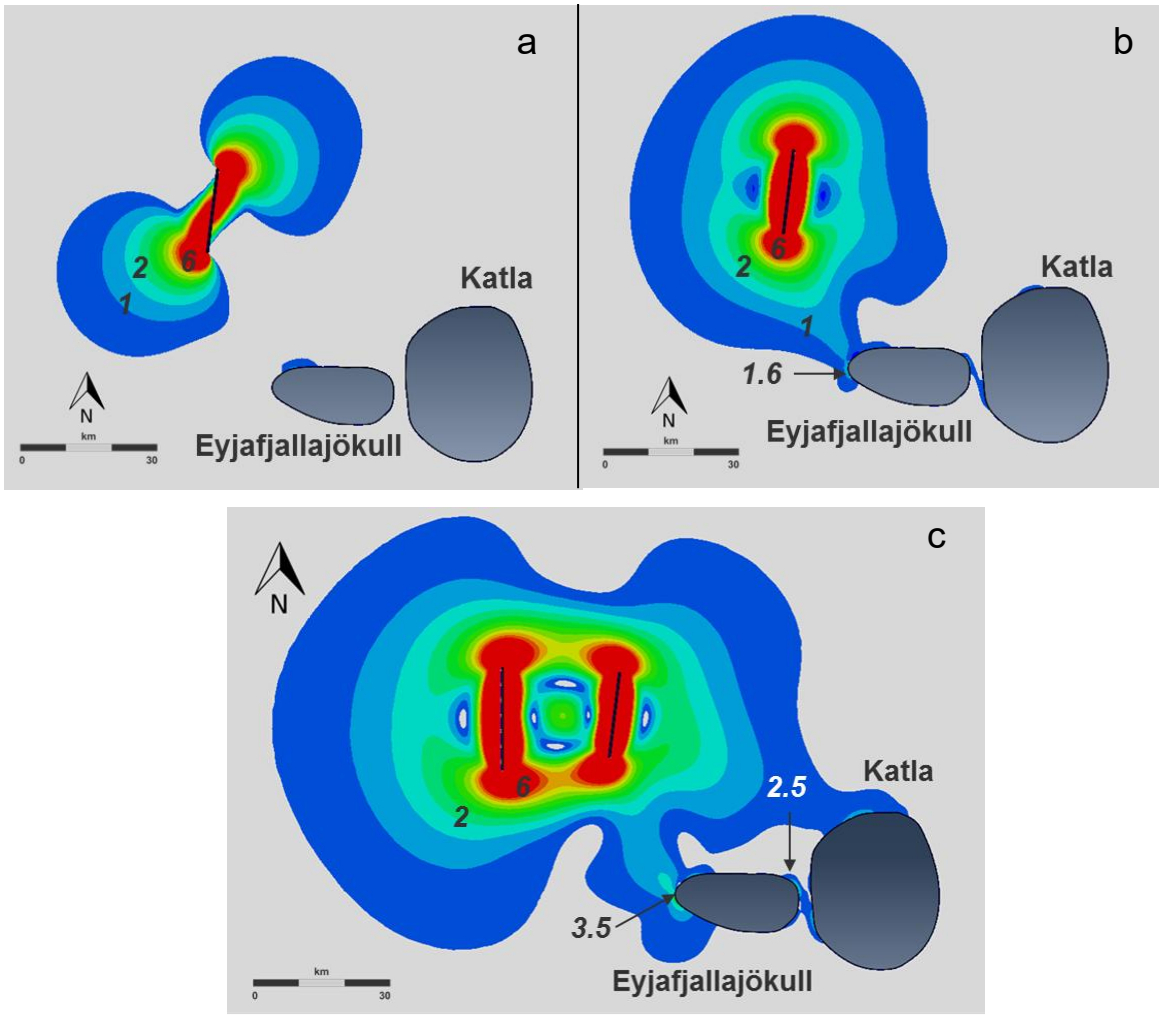

Fig. 10. Local stress effects at Eyjafjallajökull and Katla due to the June 2000 earthquakes, modelled as 20 km long faults. The loading used is stress drop of 10 MPa. a) Effect on tensile stress concentration due to slip on the 17 June fault (the Arnes Fault). Tensile stress is in the range of a fraction of a mega-pascal concentrates in the northern part of Eyjafjallajökull. b) Shear stress (von Mises) concentration due to the 17 June fault slip. Shear stress in the range of 0.1-2 MPa concentrates at Eyjafjallajökull and Katla, and particularly in the zone (the pass) between the volcanoes. c) For comparison, shear stress concentration at Eyjafjallajökull and Katla due to the combined effects of the earthquakes of 17 June and 21 June, both modelled as 20 km long faults with stress drops of 10 MPa.

Based on these data, we calculated the stress change generated by the 17 June 2000 earthquake, the so-called Arnes Fault. We focus first on this event because it is closer to Eyjafjallajökull than the 21 June 2000 event (the Hestfjall Fault). The results are shown in Fig. 10a,b. There is both shear and tensile stress concentration around the volcanoes, particularly Eyjafjallajökull, as a consequence of the slip on the Arnes Fault. The shear stress concentration is larger than the tensile stress concentration. In particular the shear stress concentrates in the pass (Fimmvörduhals) where the March 2010 effusive eruption started. The tensile stresses concentrate mainly around the northwestern side of Eyjafjallajökull.

The stress magnitudes are low - ranging from 0.1 MPa to close to 2 MPa (Fig. 8a, 8b). Yet, stresses of this magnitude, and lower, are known to have triggered earthquakes in many parts of the world. In particular, within minutes to a few hours of the earlier 2000 earthquake, on 17 June (the Arnes Fault), there were many triggered M4.5-5 earthquakes on the Reykjanes Peninsula up to a distance of 90 km from the Arnes Fault (Stefansson et al., 2003). The stress changes at these distances were certainly much less than those at Eyjafjallajökull. Also, Arnadottir et al. (2003) suggest that static stress changes of 0.1 MPa and associated with the June 17 earthquake (the Arnes Fault) many have triggered the 21 June 2000 earthquake.

We also calculated the stress effects of both the faults slipping in a dextral manner. The results (Fig. 10c) are similar to, although somewhat larger than, those obtained for a single fault. Clearly, both shear and tensile stresses concentrate at Eyjafjallajökull and at similar locations as for the single (Arnes) fault slip, and the stress concentration at Katla is much larger than that of a single fault. Thus the stress effects of faulting in the SISZ on these two volcanoes are apparently mainly due to the fault, in this case the Arnes Fault, which is closer to the volcanoes, but the slip on both faults may have contributed to the stress changes at the volcanoes.

While there is shear and tensile stress concentration at Eyjafjallajökull that can be attributed to the June 2000 earthquakes, the absolute magnitudes of these stresses are low. A related change in the local stresses, however, is that before the earthquakes occurred compressive stresses dominated in the volcano, whereas following the earthquake the compressive stresses were reduced so as to become a low tensile stress in parts of the volcano. Thus, while the compressive stresses in Eyjafjallajökull prior to the earthquakes favoured dike deflection into sills and/or dike arrest, the local stresses following the earthquakes are much more favourable to dike injections reaching the surface of the volcano.

6.3 Effects of fault slip on the local stresses: long faults

The main microseismic activity in the SISZ is confined to a zone that is about 70 km long in the east-west direction and some 10-20 km wide in the north-south direction (Fig. 1). However, faults that produce M7.1 earthquakes are generally 40-80 km long (Wells and Coppersmith, 1994), suggesting that the dextral north-northeast trending faults of the SISZ that produce such earthquakes are at least 50-60 km long (Gudmundsson, 1995a, 2007). It then follows that, during such earthquakes, the north-south width of the SISZ must be at least 50-60 km.

Numerous north-northeast striking dextral strike-slip faults and conjugate east-northeast striking sinistral faults occur in the Pleistocene rocks of South Iceland, far north of the main microseismicity zone of the SISZ (Gudmundsson, 2007, 2017). These conjugate systems indicate that ruptures can extend for tens of kilometres outside the main microseismicity zone during large earthquakes. The surface displacements in some of the earlier Holocene earthquakes have been estimated at about 2.7 m, indicating a total length of the north-south striking part of the fault of about 50 km (Bergerat et al., 2003). The estimated magnitude is then M7.1. Some of the earthquakes in South Iceland may reach at magnitudes M7.2-7.3. Based on the empirical relationship between total length and magnitude obtained by Wells and Coppersmith (1994), the maximum subsurface length of the associated faults could then be 80-100 km. The surface rupture length is less - commonly about 75% (but may be as little as 50%) of the maximum subsurface length. In this case the surface length would then be 60-75 km.

To see what effects large earthquakes in the SISZ could have on the local stresses of the nearby volcanoes - here with a focus on Eyjafjallajökull and Katla - we made numerical models with a conservative estimate of one 45-km-long and another 60-km-long N-striking dextral strike-slip faults. The 45-km-long fault extends from the central microseismic part of the SISZ to the coast (Fig. 9). By contrast, the 60-km-long fault extends from the central microseismic part of the SISZ to the erupting hot spring Geysir. Both these extensions fit with the distribution of earthquakes in South Iceland following the June 2000 earthquakes. Both faults are assumed to coincide in location with the 17 June (Arnes) 2000 fault (Fig. 9). Both fault slips may potentially occur in the future.

As indicated above, we use dynamic Young's modulus of 80 GPa for the middle part, and 130 GPa for the deeper part, of the crust. We also use Poisson's ratio of 0.25 in all the models. The measured displacements in the SISZ are as much as 2.7 m at the surface (Bergerat et al., 2003), which may be 50-75% of the maximum slip at depth (Wells and Coppersmith, 1994). Here we use the conservative displacement of 3 m, but it could easily be larger. As discussed above, we use driving shear-stress loading of 10 MPa as a likely stress drop rather than using

the slip as loading. We assume the fault to coincide with the 17 June 2000 fault (the Arnes Fault), but it could be further to the east, as in the 1912 earthquakes (Bjarnason et al. 1993), in which case the stress effects on the two volcanoes would be greater.

The results show clear fault-slip stress effects on the volcanoes. The first model (Fig. 11a,b) shows the effect of loading to slip of the 45-km-long fault. The loading is 10 MPa shear stress, that is, the stress drop is, as in the other models here, assumed 10 MPa. The results show stress concentration, both tensile and shear at both Eyjafjallajökull and Katla. The maximum shear stress at Eyjafjallajökull is quite high, or about 6 MPa, whereas the tensile stress is close to a maximum of 2 MPa. Stresses of this magnitude are known to trigger earthqukaes and may help injected dikes to reach the surface.

The second model (Fig. 11c,d) shows the effect of a 60-km-long fault extending to Geysir. When the loading is shear stress of 10 MPa, the tensile stresses concentrate mainly around Eyjafjallajökull, but the shear stresses concentration occurs both at Eyjafjallajökull and at the north and west side of the Katla volcano (Fig. 11c, d). Similar results are obtained when the loading is slip, a total of 3 m is used here, rather than stress drop. There is a clear concentration of shear and tensile stresses around Eyjafjallajökull and Katla. The tensile stresses generally favours east-west trending dikes and volcanic fissures. Understandably, there is stress concentration in many of the models (Figs. 10 and 11) in the strip of land - the pass - between the two volcanoes, namely on Fimmvörduhals where the effusive eruption of Eyjafjallajökull in March 2010 occurred.

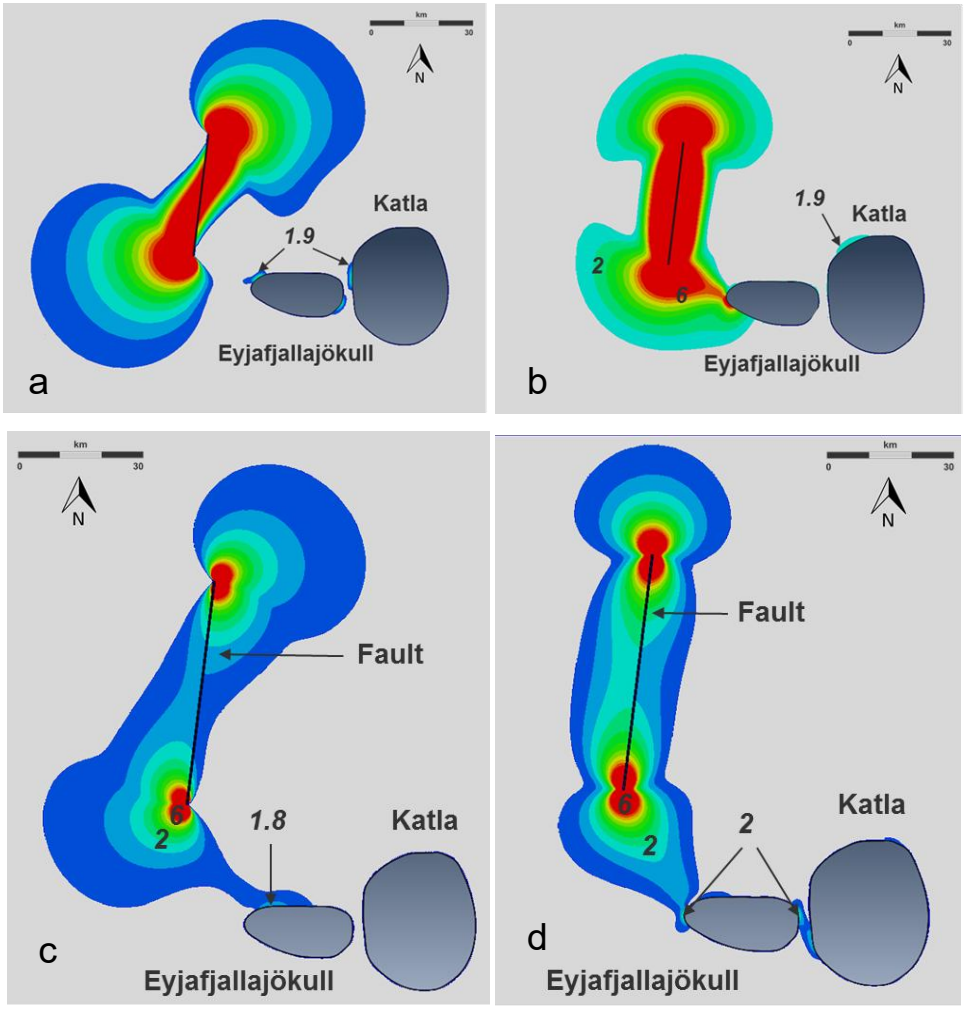

Fig. 11. Local tensile and shear stresses at Eyjafjallajökull and Katla induced by slip on long nearby dextral strike-slip faults. a) Tensile stresses induced by slip on a 45 km long fault extending from the central part of the SISZ to the coast (cf. Fig. 9). b) Shear stresses induced by the fault in a. c) Tensile stress related to slip on a 60 km long fault extending from the central part of the SISZ north to Geysir (cf. Fig. 9). d) Shear stresses related to the fault in c. In both scenarios there are considerable stress concentrations at Eyjafjallajökull and Katla - particularly Eyjafjallajökull where the stress magnitudes reach several mega-pascals.

The results (Fig. 10) show that the stress changes associated with slip on long N-striking dextral faults in the SISZ can have significant effects on the local stresses at and around the volcanoes of Eyjafjallajokull and Katla. The stress changes, based on these numerical models, agree with those obtained by the 20-km-long dextral faults analysed above (Fig. 8) and would generally encourage dikes injected into the volcanoes to reach the surface. This is in contrast with the compressive stresses transferred to these volcanoes from the SISZ during its normal loading (in the absence of large slips on north-trending dextral faults) which favour dike arrest or, alternatively, dike deflection into sills (Fig. 7b). The numerical models may thus partly explain why the there were no eruptions in Eyjafjallajokull during the doming and inferred magma emplacement in the decade before the June 2000 earthquakes. And, also, why the

magma injected into the volcano in late 2009 and early 2010 was eventually able to reach the surface and erupt.

7. Discussion

The results presented here indicate that general movement across the SISZ, as well as strong to large earthquakes in the zone, affect the local stresses in the volcanoes that are located its vicinity. This applies particularly to the volcanoes located in the quadrants closest to the seismic zone (Figs 1-7). It is clear that the stress transfer from the SISZ to the volcanoes in the quadrants favours tensile stress concentration in Hekla and compressive stress concentrations in the Hengill and Eyjafjallajökull (and Katla to a lesser degree) during the general loading of the SISZ (Figs. 2-3; Gudmundsson and Brenner, 2003). By contrast, following dextral slip on north-south striking faults in the SISZ (Fig. 9), particularly during and following strong and large earthquakes in the zone – the largest ones occurring on average once every century - tensile stresses decrease in Hekla but increase in Hengill, Eyjafjallajökull, and Katla.

Here we have modelled the tensile and compressive stresses associated with loading and fault slip in the SISZ only for Eyjafjallajökull and Katla, but similar stress changes would be expected in Hengill (Figs. 2-3). It should be noted, though, that the largest earthquakes in the western part of the SISZ are generally smaller than the largest ones in the eastern part, so that the absolute stress transfer to Hengill might, for that reason, be assumed to be somewhat smaller than that to Eyjafjallajökull. However, Hengill is much closer to the SISZ than Eyjafjallajökull, so for that reason the stress changes in Hengill during the largest earthquakes could be similar to or even larger than those in Eyjafjallajökull – and most likely much larger than those in Katla (cf. Gudmundsson and Brenner, 2003).

The results fit well with the events before the June 2000 earthquakes. There were unusually frequent eruptions in Hekla, located in a transtension quadrant, and doming in both Hengill and Eyjafjallajökull, as would be expected from their location within transpression quadrants (Figs. 1-7, 9). The frequent eruptions of Hekla are partly understandable in terms of the concentration of tensile stress in the quadrant hosting the volcano, and partly because the main eruptive fissure, the Hekla Fissure (the same one is used again and again, Fig. 5) is presumably an old east-northeast striking sinistral fault associated with the stress field of the SISZ (Gudmundsson and Brenner, 2003). However, such frequent eruptions occur only if a dike is emplaced at a suitable time and, by being only partly solidified before the next eruption takes place, maintains the weakness of the Hekla Fissure and its extension as a feeder-dike to the source magma chamber. Such a dike, we suggest, was provided by the 1970 Hekla eruption (Gudmundsson

and Brenner, 2003). Following the 1970 eruption, there were eruptions in 1980, 1981 (which may be regarded as continuation of the 1980 eruption), 1991, and 2000. The most recent eruption in Hekla occurred in February 2020, that is, just before the June 2000 earthquakes. Since the June 2000 earthquakes (and associated relaxation of tensile stress in Hekla, cf. Gudmundsson and Brenner, 2003), there have been no eruptions in Hekla.

The compressive stresses and doming in Hengill and Eyjafjallajökull can be interpreted in various ways. Since these volcanoes are located in areas of tranpression in relation to general sinistral movement across the entire SISZ, it follows that part of the doming could be related to the compressive stresses thus generated (Gudmundsson and Brenner, 2003). An alternative explanation for both volcanoes is that the doming was generated by magmatic intrusions that did not reach the surface (Feigl et al., 2000; Sigmundsson et al., 2010). Both explanations may, of course, be correct since they are complementary.

If magma intrusion took place at the time of compressive stress transfer from the SISZ, then it follows that the local stress field in Hengill and Eyjafjallajökull would be such as to encourage dike arrest or deflection into sills and discourage dike propagation to the surface to feed an eruption. Early models of magma intrusion assumed them to take the form of spherical intrusions – using Mogi models or nucleus of strains. For Hengill, the proposed spherical source was supposed to be at 7 km depth (Feigl et al., 2000). However, the proposed location of the source (Ducrocq et al., 2021) does not fit with a magma chamber that can be associated with any active composite volcano in the Hengill area. While the intrusion may have been far outside the volcano and just happened to take on a spherical form, such an interpretation is not very plausible in view of what is known about the internal structures of fossil composite volcanoes in Iceland in general (Gudmundsson, 2020).

Similarly, early interpretations of the earthquakes and uplift in Eyjafjallajökull, particularly the 1999 inflation (with a maximum uplift of about 0.35 m) placed the spherical source at 3.5 km depth but 4 km south of the summit crater of the volcano (Sturkell et al., 2003). This location is perhaps not a very likely one as regards a shallow magma chamber, and later interpretations of magma intrusion in the decade before the 2010 eruption favour sill injections at different locations (Sigmundsson et al., 2010). Again, part of the stress concentration generating the uplift and earthquakes in the decade prior to the eruption could be related to stress transfer from the SISZ (Gudmundsson and Brenner, 2003).

There are two main effects of the stress change in Eyjafjallajökull following the June 2000 earthquakes - and more so when M7 or larger earthquakes occur on dextral north-south striking faults in the vicinity of the volcano. One is the relaxation of the existing compressive stress that

builds up during stress transfer associated with the normal sinistral loading of the SISZ. Part of the strain, and therefore the stress, that had accumulated in the SISZ for decades was relaxed during the M6.6 June 2000 earthquakes and, to a lesser extent, during the M6.3 Ölfus earthquake (Sigbjörnsson et al., 2009). This relaxation means that the compressive stress that had built up inside and around Eyjafjallajökull (and Hengill) was also relaxed. The other effect is concentration of tensile stress, attributable to slip on the dextral faults, in Eyjafjallajökull (and to a lesser degree in Katla) (Figs 9 and 10). The location of Hengill in relation to the SISZ and the June 2000 earthquake faults (Figs. 1-3, 9) means that the stress changes associated with the earthquakes were different from those in Eyjafjallajökull. Also, the location of the 2008 Ölfus earthquake on a dextral fault (Sigbjörnsson et al., 2009) means that the co-seismic slip put Hengill into compressive stress rather than tensile stress.

These stress changes in Eyjafjallajökull would have allowed injected dikes to reach the surface, in the case of the March 2010 eruption, and reach the shallow magma chamber so as to trigger eruption from it in the April 2010 eruption. For the June 2000 earthquakes, the stress changes are small - of the order of a fraction of a mega-pascal. This follows partly because the closer fault (Arnes Fault) is still some 50 km from Eyjafjallajökull. However, stress changes of the order of a fraction of a mega-pascal are supposed to have triggered earthquakes, even in the SISZ. For example, Arnadottir et al. (2008) suggest that stress changes of 0.1 MPa triggered the second of the June 2000 earthquakes. Similarly, within minutes to a few hours of the 17 June 2000 (Arnes Fault) earthquake, there were many triggered M4.5-5 earthquakes on the Reykjanes Peninsula up to a distance of 90 km from the Arnes Fault (Stefansson et al., 2003). The stress chances at those distances were certainly much less than those at Eyjafjallajökull.

Given the stress changes following the June 2000 earthquakes, the question is then: Why did an eruption not occur immediately following the earthquakes? The reason is that for an eruption to occur, there must be available magma in a favourable location. The likely scenario in Eyjafjallajökull is that a new magma injection into the volcano started only in 2009 - primarily in the episode that lasted from about December 2009 to March 2010 (Sigmundsson et al., 2010). Seismic evidence, however, indicates that magma transport from the upper mantle and up into the crust below Eyjafjallajökull (at 17-29 km depth) started earlier, or in late March and April 2009, that is, approximately one year before the eruptions (Karlsdottir et al., 2012). During the continuation of this episode into March and April 2010 dikes were clearly able to propagate to the surface of the volcano in a manner that was not possible during the earlier magma injections, namely those in the decade before the 2000 earthquakes.

What happened to the magma from March 2009 until the eruptions in March and April 2010 is, as indicated above, apparently very complex; no clear and consistent picture of the magma migration story has been provided so far. The magma-migration scenarios suggested and illustrated by Sigmundsson et al. (2010), Karlsdottir et al. (2012), and Tarasewicz et al. (2012) are widely different. For example, Sigmundsson et al. (2010) show 2 sills forming just prior to the 2010 eruptions. The feeder to these sills passes through sills proposed to have formed in the doming and earthquake episodes of 1994 and 1999. For this to happen, those earlier sills must have solidified so as to behave as brittle during the feeder-dike propagation. By contrast, Tarasewicz et al. (2012) show 4 sills that are all liquid during the eruptions. These are at very different depths from the sills proposed by Sigmundsson et al. (2010). In the Tarasewicz et al. (2012) model the feeder-dike to both of the 2010 eruptions meets all the sills, but does not cut through them, and receives some magma from them on its way to the surface. In the third model (Karlsdottir et al., 2012) there are no clear major sills forming just prior to the 2010 eruptions, but rather a volume of unspecified intrusions (plus a small sill-like intrusion in one of the corners of this volume and an inclined sheet in another corner). In this model, there are two feeder-dikes, both of whom pass through the sills from the 1994 and 1999 events.

For a homogeneous, isotropic elastic half-space model, the emplacement of sills of the lateral dimensions indicated in some of the models above suggests that the measured uplifts of the volcano should be of the order of many metres. Based on classical elastic crack theory (e.g. Gudmundsson, 2011) a sill that has lateral dimensions of 10-20 km should have a thickness of at least 10-20 m - and commonly much more. While part of the space generate for such a sill could be thorough down-bending of the layers below the sill, a large part, in the present case, would be expected to be generated through up-bending or doming of the layers above the sill (Gudmundsson, 2011). It follows that uplift or doming of the order or metres or more would be expected for such sills. The maximum measured uplifts, however, were about 0.35 m for the large sills inferred to have formed in the 1990s (Sturkell et al., 2010).

Since all these models are based on basically the same data (primarily earthquakes and surface deformation), their differences may indicate how difficult it is to trace magma paths through dikes and sills even in very well-monitored volcanoes. Part of the difficulty may relate to the modelling methods. Eyjafjallajökull and the crustal segments to which the volcano belongs is composed of very heterogeneous rocks. The exposed part of the volcano itself consists of layers and units (Fig. 7b), such as basaltic sills, inclined sheets, dikes, hyaloclastites, sediments, scoria layers, and other layers and units that have widely different mechanical properties. During any loading, say from the SISZ and/or through magma intrusion, the

different layers respond differently (depending on their stiffness), and there will be stress concentrations (raised stresses) at contacts between dissimilar rock units and layers. Any attempt to model the deformation in such a volcano through homogeneous, isotropic elastic half-space techniques is bound to be difficult and yield variable results. A further approach would be to consider the mechanical anisotropy and layering in the volcano, at least for the part that is easily observed at the surface (Fig. 7), so as to obtain results that are internally consistent and constrained by direct observations.

8. Summary and conclusions

Seismogenic faulting in the vicinity of fluid-filled reservoirs and elastic inclusions of various kind (including volcanoes) affects the local stresses around the reservoirs/inclusions. One of the two most active earthquake zones in Iceland is the South Iceland Seismic Zone (SISZ) which also happens to have volcanoes located at three of its four quadrants (Figs 1-3, 9). During loading of the SISZ stresses are transferred to these nearby volcanoes which act partly as elastic inclusions and, for those that have magma chambers, partly as fluid-filled reservoirs. Simple numerical models show that the general loading from the SISZ results in transpression, that is, in the concentration of compressive stresses in two of these volcanoes, namely in Hengill and Eyjafjallajökull, and concentration of tensile stresses in Hekla. Hengill was subject to doming with numerous earthquakes in 1990's but has been mostly quiet following the June 2000 earthquakes. A smaller earthquake, of magnitude 6.3 on a dextral, north-south striking and 14-km-long fault, occurred at the western end of the SISZ in May 2008 (Sigbjörnsson et al., 2009). This earthquake extended into the Hengill area, but was about 7 km east of Hengill itself. The displacements associated with this earthquake put Hengill into a transpressive regime again.

Eyjafjallajökull was mostly quiet following the June 2000 earthquakes until about December 2009 when magma injection into the roots of the volcano was detected. There was seismic evidence for magma movement at the crust-mantle boundary beneath Eyjafjallajökull from the spring of 2009. The compressive stress relaxation (and some the buildup of tensile stress) in the upper crust and in the volcano itself was presumably one of the main reasons why magma was able to reach the surface and erupt twice in Eyjafjallajökull in 2010. By contrast, the relaxation of tensile stress in and around Hekla during and following the June 2000 earthquakes may be one reason why it has not erupted now for a quarter of a century but erupted 4 times in the quarter of a century before the June 2000 earthquakes.

The main conclusions of this study may be summarised as follows:

1. Observational and theoretical results indicate that there is a strong mechanical interaction between the SISZ and its nearby volcanoes. In particular, this applies to the volcanoes Hekla, Hengill, and Eyjafjallajökull and, to a lesser degree, Katla. The first three of these volcanoes are located at (Hekla and Hengill) or close to (Eyjafjallajökull) the quadrants of stress concentration associated with the general sinistral east-west movement across the SISZ (Figs. 1-3).
2. During normal sinistral displacement across the SISZ, Hekla concentrates relative tensile stresses (it is located in a quadrant of transtension), whereas Hengill and Eyjafjallajökull concentrate relative compressive stresses (they are located in a quadrants of transpression). Thus, Hengill and Eyjafjallajökull are subject to compressive stresses that may generate doming (uplift) and earthquakes with or without magma intrusion. In the case of magma intrusion, there would be a strong tendency for any dikes injected into these two volcanoes to become arrested, and some deflected into sills, at contacts between mechanically dissimilar layers inside the volcanoes due to compressive stresses induced by the general sinistral movement across the SISZ (Figs 1-3). These scenarios were, indeed, observed in Hengill and Eyjafjallajökull prior to the June 2000 earthquakes.
3. Strong to large earthquakes in the SISZ, primarily on northerly striking dextral strike-slip faults, however, induce stress relaxation in the nearby volcanoes. This relaxation results in reduced compressive stresses in the volcanoes located in the quadrants of transpression. In addition to the compressive stress relaxation, there was tensile stress concentration in Eyjafjallajökull (and to a lesser degree in Katla) following the 2000 earthquakes. By contrast, the 2008 (M6.3) Ölfus earthquake caused renewed transpression in Hengill.
4. If magma intrusion takes place during compressive stress relaxation, relative tension, in these volcanoes, then eruptions may be expected to occur. This is exactly what happened in Eyjafjallajökull in 2010. In the 1990's there were apparently several magma intrusions into the roots of Eyjafjallajökull, but all the potential feeder-dikes became deflected into sills and/or arrested at depth in the volcano. This, we suggest, is partly related to the high horizontal compressive stresses that existed in the volcano due to the normal loading and stress transfer from the SISZ. By contrast, in 2009 when new magma intrusions took place in Eyjafjallajökull, the changed stress field (the relative tension) made it possible for the dikes to reach the surface of the volcano in two eruptions, namely the March 2010 flank eruption and the April 2010 summit eruption.

5. The results emphasise the importance of stress transfer between seismic zones and nearby volcanoes. Since all active plate boundaries worldwide - divergent, convergent and (to a lesser degree) transform boundaries - are characterised by concurrent activity in seismic zones and nearby volcanoes, it follows that an interaction of the type illustrated here for South Iceland is likely to be common. The results of the present paper should thus help bring into research focus the common mechanical interactions between seismogenic fault zones and nearby active volcanoes.

Acknowledgements. Some of the results presented here derive from various projects on the mechanics of earthquakes and volcanic eruptions, focusing on Iceland. These projects have been funded by the Icelandic Science Foundation, the Research Council of Norway, the Volkswagen Foundation in Germany, the Natural Environmental Research Council of the United Kingdom, and the European Research Council.

References

Ambraseys, N.N., Jackson, J.A., 1998. Faulting associated with historical and recent earthquakes in the eastern Mediterranean region. Geophys. J. Int. 133, 390–406.

Andrew, R.E.B., Gudmundsson, A., 2008. Volcanoes as elastic inclusions: their effects on the propagation of dykes, volcanic fissures, and volcanic zones in Iceland. Journal of Volcanology and Geothermal Research, 177, 1045-1055.

Angelier, J., Bergerat, F. 2002. Behaviour of the 21 June 2000 earthquake in South Iceland as revealed in an asphalted car park. J. Struct. Geol. 24, 1925-1936.

Angelier, J., Bergerat, F., Bellou, M. & Homberg, C. 2004a. Co-seismic strike-slip fault displacement determined from push-up structures: the Selsund Fault case, South Iceland. J. Struct. Geol. 26, 709-724.

Angelier, J., Slunga, R., Bergerat, F., Stefansson, R., Homberg, C. 2004b. Perturbation of stress and oceanic rift extension across transform faults shown by earthquake focal mechanisms in Iceland. Earth Planet. Sci. Lett. 219, 271-284.

Arnadottir, T., Geirsson, H., Jiang, W., 2008. Crustal deformation in Iceland: Plate spreading and earthquake deformation. Jökull, 58, 59-74.

Arnadottir, T., Haines, J., Geirsson, H., Hreinsdottir, S., 2018. A preseismic strain anomaly detected before the M6 earthquakes in the South Iceland Seismic Zone from GPS station velocities. J. Geophys. Res., 123, 11,091-11,111. doi.org/org/10.1029/2001GL013332.

Belardinelli, M.E., Bonafede, M., Gudmundsson, A. 2000. Secondary earthquake fractures generated by a strike-slip fault in the South Iceland Seismic Zone. J. Geophys. Res. 105, 13,613-13,629.

Bergerat, F. 2001. Historical seismicity in Iceland: geological aspects, environmental and social impacts. Examples in the South Iceland Seismic Zone. C. R. Geoscience 333, 81-92.

Bergerat, F., Angelier, J. 2001. Mechanisms of the faults of 17 and 21 June 2000 earthquakes in the South Iceland Seismic Zone from the surface traces of the Arnes and Hestfjall faults. C. R. Geoscience 333, 35-44.

Bergerat, F., Angelier, J. 2003. Mechanical behaviour of the Arnes and Hestfjall Faults of the June 2000 earthquakes in Southern Iceland: inferences fro the surface traces and tectonic model. J. Struct. Geol. 25, 591-609.

Bergerat, F., Gudmundsson, A., Angelier, J., Rögnvaldsson, S. T. 1998. Seismotectonics of the central part of the South Iceland Seismic Zone. Tectonophysics 298, 319-335.

Bergerat, F., Angelier, J., Gudmundsson, A., Torfason, H. 2003. Push-ups, fracture patterns, and palaeoseismology of the Leirubakki Fault, South Iceland. J. Struct. Geol. 25, 591-609.

Bjarnason, I. T., Cowie, P., Anders, M. H., Seeber, L., Scholz, C. H. 1993. The 1912 Iceland earthquake rupture - growth and development of a nascent transform system. Bull. Seismol. Soc. Am. 83, 416-435.

Clifton, A., Einarsson, P. 2005. Styles of surface rupture accompanying the June 17 and 21 2000 earthquakes in the South Iceland Seismic Zone. Tectonophysics 396, 141-159.

Decriem, J., Arnadottir, T., 2012. Transient crustal deformation in the South Iceland Seismic Zone observed by GPS and InSAR during 2000-2008. Tectonophysics, 581, 6-18.

Ducrocq, C., Geirsson, H., Arnadottir, T. et al., 2021. Inflation-deflation episodes in the Hengill and Hrodmundartindur volcanic complexes, SW Iceland. Front. Earth Sci., 9, doi: 10.3389/feart.2021.725109.

Einarsson, P., 2008. Plate boundaries, rifts and transforms in Iceland. Jökull, 58, 35-58.

Feigl, K.L., Gasperi, J., Sigmundsson, F., Rigo, A., 2000. Crustal deformation near Hengill volcano, Iceland 1993-1998: Coupling between magmatic activity and faulting inferred from elastic modeling of satellite radar interferograms J. Geophys. Res., 105, 25,655-25,670.

Galindo, I., Gudmundsson, A., 2012. Basaltic feeder dykes in rift zones: geometry, emplacement, and effusion rates. Nat. Hazards Earth Syst. Sci., 12, 3683–3700.

Geirsson, H., LaFemina, P., Arnadottir, T., Sturkell, E., Sigmundsson, F., Travis, M., Schmidt, P., Lund, B., Hreinsdottir, S., Bennet, R., 2010. Volcano deformation at active plate boundaries: deep magma accumulation at Hekla volcano and plate boundary deformation in South Iceland. J. Geophys. Res., 117, doi: 10.1029/2012JB009400.

Gislason, S.R., Hassenkam, T., Nedel, S., Bovet, N., Eiriksdottir, E.S., Alfredsson, H.A., Hem, C.P., Balogh, Z.I., Dideriksen, K., Oskarsson, N., Sigfusson, B., Larsen, G., Stipp, S.L. S., 2011. Characterization of the Eyjafjallajökull volcanic ash particles and a protocol for rapid risk assessment. PNAS, 108, 7307-7312.

Gudmundsson, A., 1988. Effect of tensile stress concentration around magma chambers on intrusion and extrusion frequencies. Journal of Volcanology and Geothermal Research, 35, 179-194.

Gudmundsson, A. 1995a. Ocean-ridge discontinuities in Iceland. J.Geol. Soc. Lond. 152, 1011-1015.

Gudmundsson, A., 1995b. Infrastructure and mechanics of volcanic systems in Iceland. J. Volcanol. Geotherm. Res., 64, 1-22.

Gudmundsson, A., 2007. Infrastructure and evolution of ocean-ridge discontinuities in Iceland. J. Geodyn., 43, 6-29.

Gudmundsson, A., 2011. Rock Fractures in Geological Processes. Cambridge University Press, Cambridge.

Gudmundsson, A., 2017. Glorious Geology of Iceland's Golden Circle. Springer-Nature, Berlin.

Gudmundsson, A., 2022. The propagation paths of fluid-driven fractures in layered and faulted rocks. Geological Magazine, 159, 1978-2001, doi.org/10.1017/S0016756822000826

Gudmundsson, A. 2025a. Statistical physics of fissure swarms and dike swarms. Geosciences (in press).

Gudmundsson, A., 2025b. The effects of stress gradients on faulting and dike emplacement, with applications to Santorini and Iceland. In: The Role of Tectonics on the Emergence and Evolution of Volcanic Features with Particular Reference to the Mediterranean Region. Geol. Soc. Lond. Spec. Publ. (in press).

Gudmundsson, A., 2025c Multiple dikes make eruptions easy. J.Volcanol. Geotherm. Res., 460, https://doi.org/10.1016/j.jvolgeores.2025.108284

Gudmundsson, A., Brenner, S. L. 2003. Loading of a seismic zone to failure deforms nearby volcanoes: a new earthquake precursor. Terra Nova 15, 187-193.

Gudmundsson, A., Oskarsson, N., Gronvold, K., Saemundsson, K., Sigurdsson, O., Stefansson, R., Gislason, S.R., Einarsson, P., Brandsdottir, B., Larsen, G., Johannesson, H., Thordarson, T., 1992. The 1991 eruption of Hekla, Iceland, Bull. Volcanol., 54, 238-246.

Gudmundsson, A.T., 2001. Icelandic Volcanoes. Vaka-Helgafell, Reykjavik (in Icelandic).

Gudmundsson, M.T., Thordarson, T., Hoskuldsson, A., Larsen, G., Bjornsson, H., Prata, F.J., Oddson, B., Magnusson, E., Hognadottir, T., Petersen, G.N., Hayward, C.L., Stevenson, J.A., Jonsdottir, J., 2012. Ash generation and distribution from the April-May 2010 eruption of Eyjafjallajökull, Iceland. Sci. Reports, 2, 572, doi: 10.1038/srep00572.

Hench, M., Lund, B., Arnadottir, T., Brandsdottir, B., 2016. Temporal stress changes associated with the 2008 Mw 6 earthquake doublet in western South Iceland Seismic Zone. Geophys. J. Int., 204, 544-554. doi.org/10.1093/gji/ggv465.

Hjaltadottir, S., Vogfjord, K.S., 2005. Subsurface fault mapping in Southwest Iceland by relative location of aftershocks of the June 2000 earthquakes. Report of the Icelandic Met Office, VI-ES-01, Reykjavik.

Hobe, A., Gudmundsson, A. Selec, B., et al. 2025. Tomographic and volcanotectonic control on the 2021–2023 Fagradalsfjall eruptions, Iceland. Sci. Rep., 15, https://doi.org/10.1038/s41598-025-95169-6.

Jakobsdottir, S.S., 2008. Seismicity in Iceland: 1994-2007. Jökull, 58, 75-100.

Jakobsson, S.P., 1979. Outline of the petrology of Iceland. Jökull, 29, 57-73.

Kanamori, H., Anderson, D.L., 1975. Theoretical basis of some empirical relations in seismology. Seismol. Soc. Am. Bull., 65, 1073-1095.

Karlsdottir, S., Gylfason, A.G., Hoskuldsson, A., Brandsdottir, B., Ilyinskaya, E., Gudmundsson, M.T., Hognadottir, T., 2012. The 2010 Eyjafjallajökull eruption, Iceland. Icelandic Met Office, Report to ICAO, June 2012, Reykjavik.

Kusumoto, S., Gudmundsson, A., Simmenes, T.H., Geshi, N., Philipp, S. L., 2013. Inverse modeling for estimating fluid-overpressure distributions and stress intensity factors from an arbitrary open-fracture geometry. J. Struct. Geol., 46, 92-98.

Luxley, P., Blondel, P., Parson, L.M., 1997. Tectonic significance fo the South Iceland Transform Zone. J. Geophys. Res., 102, 17,967-17,980.

Parameswaran, R.M., Thorbjarnardottir, B.S., Stefansson, R., Bjarnason, I.Th., 2020. Seismicity on conjugate faults in Ölfus, South Iceland: case study of the 1998 Hjalli-Ölfus earthquake. J. Geophys. Res., 125, e2019JB019203. https://doi.org/10.1029/2019JB019203.

Parameswaran, R.M., Bjarnason, I.Th., Thorbjarnardottir, B.S., 2023. Evolution of stresses over conjugate faults in Hjalli-Ölfus, South Iceland. J. Geophys. Res., 128, e2022JB026201. https://doi.org/10.1029/2022JB026201.

Passerini, P., Marcucci, M., Sguazzoni, G., Pecchioni, E., 1997. Longitudinal strike-slip faults in ocean rifting: a mesostructural study from western to southwestern Iceland. Tectonophysics, 269, 65-89.

Pedersen, R., Jonsson, S., Arnadottir, T., Sigmundsson, F., Feigl, K. 2003. Fault slip distribution of two June 2000 M(w) 6.5 earthquakes in South Iceland estimated from joint inversion of InSAR and GPS measurements. Earth Planetary Sci. Lett. 213, 487-502.

Perlt, J., Heinert, M., 2006. Kinematic model oft he South Iceland tectonic system. Geophys. J. Int., 164, 168-175.

Rögnvaldsson, S.T., 1994. Microearthquakes in South Iceland: fault plane solutions and relative locations. PhD Thesis, Uppsala University, Uppsala.

Rögnvaldsson, S.T., (and 17 coauthors), 1998. Earthquake Swarm in Olfus in November 1998. Iceland Meteorological Office, Report VI-G98046-JA09, Reykjavik (in Icelandic).

Saemundsson, K., 1996. Hengill. Ferdafelag Islands, Reykjavik (in Icelandic).

Scholz, C. H., 2002. The Mechanics of Earthquakes and Faulting, 2nd. Ed. Cambridge University Press, Cambridge.

Sigbjörnsson, R., Snæbjörnsson, J.T., Higgins, S.M., Halldórsson, B., Ólafsson, S., 2009. A note on the Mw 6.3 earthquake in Iceland on 29 May 2008 at 15: 45 UTC. Earthquake Engng. 7, 113-126

Sigmundsson, F., Einarsson, P., Rognvaldsson, S.T., Foulger, G.R., Hodgkinson, K.R., Thorbergsson, G., 1997. The 1994-1995 seismicity and deformation at the Hengill triple junction, Iceland: triggering of earthquakes by minor magma injection in a zone of horizontal shear stress. J. Geophys. Res., 102, 15,151-15,161.

Sigmundsson, F., Hreinsdottir, S., Hooper, A., Arnadottir, T., Pedersen, R., Roberts, M.J., Oskarsson, N., Aurlac, A., Decriem, J., Einarsson, P., Geirsson, H., Hensch, M., Ofeigsson, B.G., Sturkell, E., Sveinbjornsson, H., Feigl, K., 2010. Intrusion triggering of the 2010 Eyjafjallajökull eruption. Nature, 468, 426-430.

Smith, M., 2009. ABAQUS. Standard User Manual. Version 6.9. Dassault Systemes Simulia Corp., Providence, RI (USA).

Solnes, J., Sigmundsson, F., Bessason, B., 2013. Natural Hazards in Iceland: Volcanic Eruptions and Earthquakes. Haskolautgafan, Reykjavik, 785pp (in Icelandic).

Stefansson, R., Bodvarsson, R., Slunga, R., Einarsson, P., Jakobsdottir, S., Bungum, H., Gregersen, S., Havskov, J., Hjelme, J., Korhonen, H. 1993. Earthquake Prediction Research in the South Iceland Seismic Zone and the Sil Project. Bull. Seismol. Soc. Am. 83, 696-716.

Stefansson, R., Gudmundsson, G. B., Halldorsson, P. 2000. The two large earthquakes in the South Iceland seismic zone on June 17 and 21, 2000. Report of the Iceland Met Office, Reykjavik.

Stefansson, R., Gudmundsson, G.B., Halldorsson, P., 2003. The South Iceland earthqukakes 2000 - a challenge for earthquake prediction research. Icelandic Met Office Report 03017, Reykjavik.

Steigerwald, L., Einarsson, P., Hjartardottir, A.R., 2020. Fault kinematics at the Hengill triple junction, SW-Iceland, derived from surface fracture pattern. J. Volcanol. Geotherm. Res., 391, https://doi.org/10.1016/j.jvolgeores.2018.08.017.

Sturkell, E., Sigmundsson, F., Einarsson, P., 2003. Recent unrest and magma movments at Eyjafjallajökull and Katla volcanoes, Iceland. J. Geophys. Res., 108 (B8), 2369.

Sturkell, E., Einarsson, P., Sigmundsson, F., Hooper, A., Ofeigsson, B. G., Geirsson, H., Olafsson, H., 2010. Katla and Eyjafjallajökull volcanoes. Dev. Quat. Sci., 13, 5-21.

Tarasewicz, J., White, R.S., Woods, A.W. et al., 2012. Magma mobilization by downward-propagating decompression of the Eyjafjallajökull volcanic plumbing system. Geophy. Res. Lett., 39, https://doi.org/10.1016/j.jvolgeores.2018.08.017.

Thorbjarnardottir, B.S., Bjarnason, I.Th., Stefansson, R., 2018. Seismotectonics and triggered earthquakes in the Geysir area in Iceland. EGU 2018 General Assembly, Vienna, p. 15567.

Thordarson, T., Larsen, G., 2007. Volcanism in Iceland in historical time: volcano types, eruption styles and eruptive history. Journal of Geodynamics 43, 118–152.

Thordarson, T., Höskuldsson, A., 2008. Postglacial volcanism in Iceland. Jökull, 58, 197-228.

Thordarson, T., Höskuldsson, A., 2014. Iceland. Classical Geology of Europe 3, 2nd ed. Dunedin, London.

Wells, D. and K. Coppersmith, 1994. New empirical relationships among magnitude, rupture length, rupture width, rupture area, and surface displacement. Bull. Seismol. Soc. Am., 84, 974-1002.